N69-40075

Interim Technical Report

REDUCING MULTIPATH ERROR IN AN
ANGLE-MEASURING NAVIGATION SATELLITE SYSTEM

by

Richard A. Hrusovsky

September 1969

CASE FILE COPY

Prepared for

NATIONAL AERONAUTICS AND SPACE ADMINISTRATION
Space Applications Programs Office
Washington, D. C.   20546

by

University of Pennsylvania
THE MOORE SCHOOL OF ELECTRICAL ENGINEERING
Philadelphia, Pennsylvania   19104

Moore School Report No.:   70-07

ACKNOWLEDGEMENTS

University of Pennsylvania

THE MOORE SCHOOL OF ELECTRICAL ENGINEERING

REDUCING MULTIPATH ERROR IN AN
ANGLE-MEASURING NAVIGATION SATELLITE SYSTEM

Abstract: A major error in navigational position fixing
using a satellite-borne interferometer is due to multi-
path propagation. Reflections, principally from the
earth's surface, contaminate the phase measurement which
provides positional information. A signal design method
of reducing multipath error is investigated wherein the
navigation signals are swept in frequency. A time averag-
ing of the frequency-swept signals at the navigation re-
ceiver can then be used to reduce the multipath error
contribution below the maximum fixed-frequency error.
Allowing a maximum integration time of one second calls
for a sweep rate of about 16 KHz. For certain critical
values of sweep width the multipath error may be complete-
ly cancelled. Shifts in these critical sweep width opera-
ting points due to user motion during the time interval
of integration can be tolerated at the expense of a larger
total sweep width. This is because the error, as well as
possessing numerous small zeros, has maxima which decrease
linearly with sweep width becoming sufficiently small with

large (eg. 3.2 MHz at L-band) sweep to make the precision of electrical phase-measuring equipment the limiting error factor.

Since electrical phase is path length as well as wavelength dependent, the motion of a navigating user can be substituted for the transmitter sweeping. For a one second integration time, a supersonic transport on a transatlantic flight can measure his position to within about 2.8 km using the integration-while-in-motion technique. Using the frequency sweep technique, this can be reduced to 57 m or less assuming the associated electrical phase can be measured with sufficient accuracy. The integration-while-in-motion technique requires less equipment, but a slow moving user cannot use this method for rapid position determination. Although the integration-while-in-motion method may be suitable in certain applications, a greater degree of control in error reduction is possible with the frequency sweep technique.

TABLE OF CONTENTS

1.0 INTRODUCTION

Many communications systems involve environments in which direct signals are accompanied by their indirect, time-delayed counterparts due to new and longer propagation paths created by reflection. These unwanted reflections combine with the desired direct signal to produce a contaminated composite signal and an associated system error. Of particular interest is the multipath encountered in earth-space navigation links where the multipath error can be a limiting factor in achieving required system performance.

Satellite navigation systems have been proposed in response to a growing need by long-range, high speed aircraft for more accurate position determination over oceans and land areas lacking ground stations within line-of-sight. Of most immediate concern is the heavily traveled North Atlantic corridor whose annual number of jet flights by 1975 is expected to more than double the 1964 transatlantic air traffic.[1] Satellites carrying navigation instrumentation represent all-weather systems which, for example, can provide over-ocean position fixes allowing a narrowing of air corridors to accommodate increased traffic without sacrificing safety.

One technique for radionavigation by satellite involves the measurement of angles between the navigating user and orbiting interferometers. Studies of applications of this principle have been made by Westinghouse[2-7] Cubic Corporation[8-10] and the University of Pennsylvania.[11] All of these studies reveal that multipath propagation is a major source of error. Reference 11, discussing the radiating satellite interferometer, indicates the need for a magnitude of error reduction equivalent to suppressing the multipath signal below the direct signal by as much as 47 dB to achieve position accuracies to within one nautical mile.

This work is aimed at reducing the error due to multipath in navigation systems employing satellite-borne interferometers which locate navigating users by making angular measurements. Such systems require only a single satellite to determine a position fix for navigating users in the satellite's field of view. In practice the satellite would carry a pair of crossed interferometers each of which provides a line of position along which the navigating user may be located. The intersection of these two lines of position pinpoints the user's exact location provided his altitude is known.

The angular position determination provided by an interferometer is directly related to the electrical phase difference between the signals arriving at its spaced antennas. When multipath propagation occurs, an incoming direct signal is contaminated by unwanted reflections. The phase difference measurement made on this composite signal is generally different from that of the direct signal alone. Hence the angular position of the source of incident radiation computed from this measurement is in error.

The received phase of continuous wave navigation signals propagated over a distance is both wavelength and path length dependent. The signal design schemes herein examined exploit these properties to achieve multipath error reduction. By varying the wavelength of the transmitted navigation signal and subsequently low-pass filtering at the receiving end, phase error due to multipath is generally reduced below the maximum fixed-frequency error. If the user is moving, the multipath contaminated phase measurement will undergo a variation with changing propagation path lengths due to this motion. This is a second usable mechanism for which appropriate filtering at the receiving end will result in error reduction.

Although these techniques for improvement are generally applicable, the case where the multipath signal amplitude is much less than the direct signal amplitude is chosen to demonstrate the error reduction principles. Other cases are not readily amenable to the same degree of quantitative analysis. Where necessary for the purpose of clarification, the system parameters such as satellite and user altitudes, interferometer baselines, and operating frequency are fixed or restricted in accordance with practical considerations. An insight into these considerations is provided by section 2 describing the general operation of navigation satellite systems which will benefit from multipath error reduction.

Section 3 derives the angle-measurement system phase-error equation. This is followed in the fourth section by an analysis of the proposed error reducing mechanisms applied to the results of section 3. The last section reviews the error reduction analysis and presents conclusions based on a discussion of the results of this work.

2.0   THE INTERFEROMETER NAVIGATION SATELLITE

The basic principles involved in angle-measure-ment positioning by satellite as well as methods of incorporating them into a practical navigation sys-tem are outlined below. The discussion gives an understanding of what parameter values might be used in an operational system so that the error due to the occurrence of multipath can later be assessed and processed for reduction.

2.1   System Concepts

The interferometer navigation satellite carries spaced antennas which are considered in pairs for the purpose of measuring the difference in phase of a signal incident upon them. Consider Figure 1. From the law of cosines,

$$\ell_1^2 = \frac{D^2}{4} + S^2 - DS \cos \theta$$

Similarly,

$$\ell_2^2 = \frac{D^2}{4} + S^2 - DS \cos(180° - \theta)$$

$$= \frac{D^2}{4} + S^2 + DS \cos \theta$$

SATELLITE

ANTENNA 1

$\frac{D}{2}$

$\frac{D}{2}$

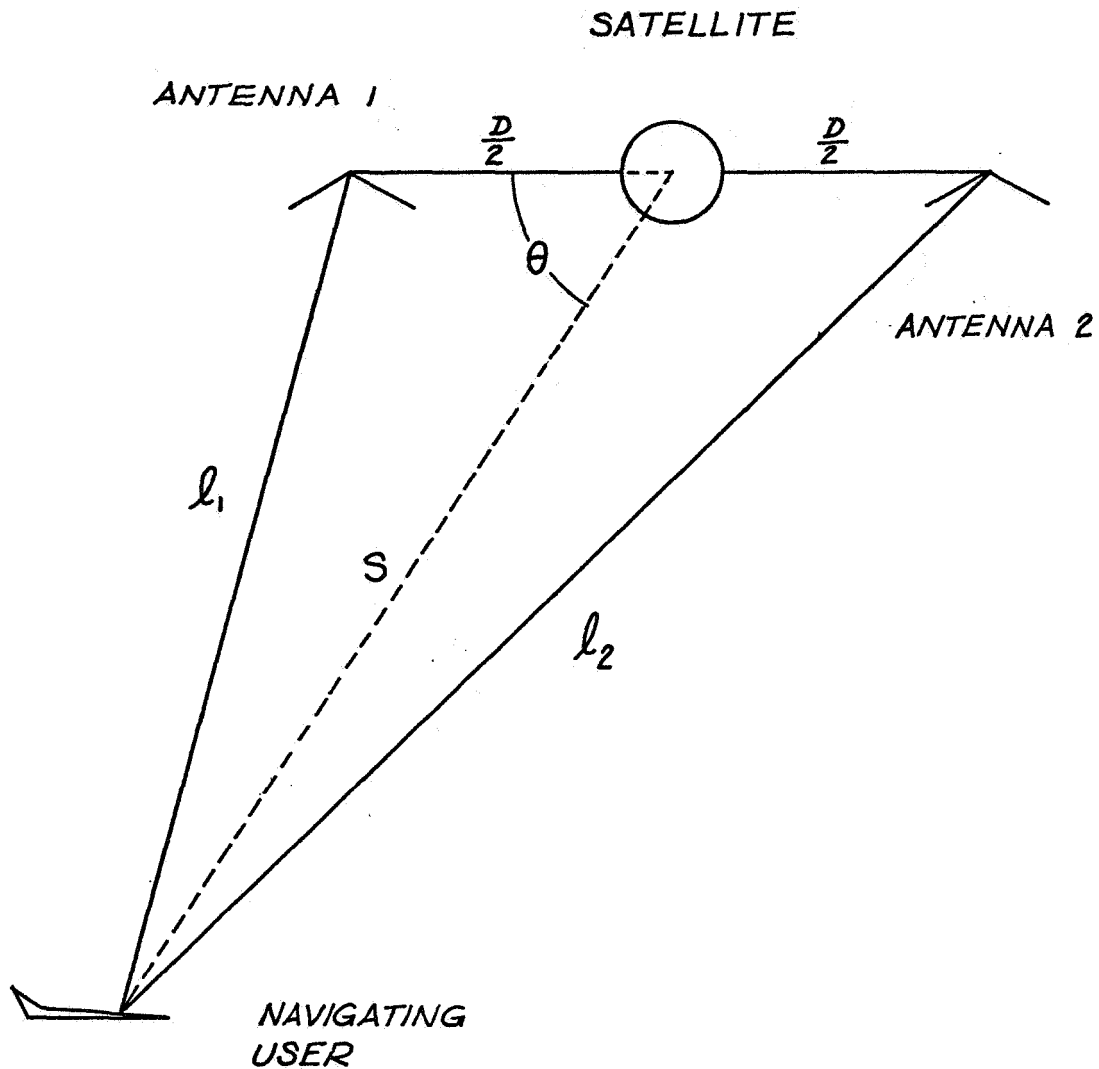θ

ANTENNA 2

ℓ_1

S

ℓ_2

NAVIGATING
USER

FIGURE 1 — GEOMETRY SHOWING POSITION
LOCATION AS MEASURED BY
THE SATELLITE INTERFEROMETER

$$\ell_2^2 - \ell_1^2 = 2DS \cos \theta$$

or
$$\ell_2 - \ell_1 = \frac{2DS \cos \theta}{\ell_1 + \ell_2}$$

For $S \gg D$, $2S \approx \ell_1 + \ell_2$ which gives

$$\ell_2 - \ell_1 = D \cos \theta$$

Converting this path length difference to difference of phase $\Delta\phi$,

$$\Delta\phi = \frac{2\pi D}{\lambda} \cos \theta \quad radians \qquad (1)$$

where λ is the operating wavelength. From the measured phase difference $\Delta\phi$ equation (1), the interferometer equation, gives θ thereby providing an angular line of position to the navigating user with respect to the interferometer baseline. A second pair of antennas with baseline perpendicular to the first is needed to pinpoint the user assuming he knows his altitude.

After differentiating equation (1),

$$\delta(\cos \theta) = \frac{\delta(\Delta\phi)}{2\pi \left(\frac{D}{\lambda}\right)} \qquad (2)$$

Equation (2) states that for a given phase measurement error, the error in determining the user's position (in terms of $\cos \theta$) is inversely proportional to D/λ , the number of wavelengths in the interferometer baseline. On the basis of (2) alone, best accuracy is obtained with D/λ as large as physically possible, perhaps 100.* However for $D/\lambda > 1$ the determination of θ can be ambiguous. This stems from the fact that measured phase differences are modulo 2π. Only if the actual phase difference (including a knowledge of which antenna phase lags) were known could a unique θ be determined from the interferometer equation. Considering (1), it is seen that for

$$D/\lambda < \left| \frac{1}{\cos \theta} \right| , \quad |\Delta\phi| < 2\pi$$ and actual phase difference equals phase difference modulo 2π. For

$$D/\lambda > \left| \frac{1}{\cos \theta} \right| \geq 1 ,$$ the actual phase difference can exceed 2π and phase measurements corresponding to more than one user location (more than one θ) can register the same phase modulo 2π.

___

*   This assumes a single-satellite interferometer. It may be possible to operate a large baseline system using two one-antenna satellites or a single one-antenna satellite allowed to synthesize a baseline along its orbital path.[12]

Presently there are four frequency bands which may be considered promising candidates for international use by airborne, satellite-borne, and ground based electronic aids to navigation: 118-132, 1540-1660, 5000-5250, and 15,400-15,700 MHz. At all these frequencies, considering the size of commonly used antennas, D/λ will probably have to exceed 1. Resolution of ambiguities may be accomplished by making measurements at two frequencies or at two different antenna spacings.[13]

One of the advantages of the interferometer navigation satellite over non - angle-measurement systems is the fact that only a single satellite need be used to obtain a position fix for users in the satellite's field of view. The use of such a satellite at synchronous altitude (36,000 km) allows continuous availability of the satellite to a given field of view and three satellites would provide complete earth coverage except for the poles. For a satellite at synchronous altitude, Figure 2 shows the minimum spacing between ambiguous lines of position for a practical range of D/λ.

There are several approaches to administering an interferometer-satellite navigation system. The possibilities for accommodating many users, process-
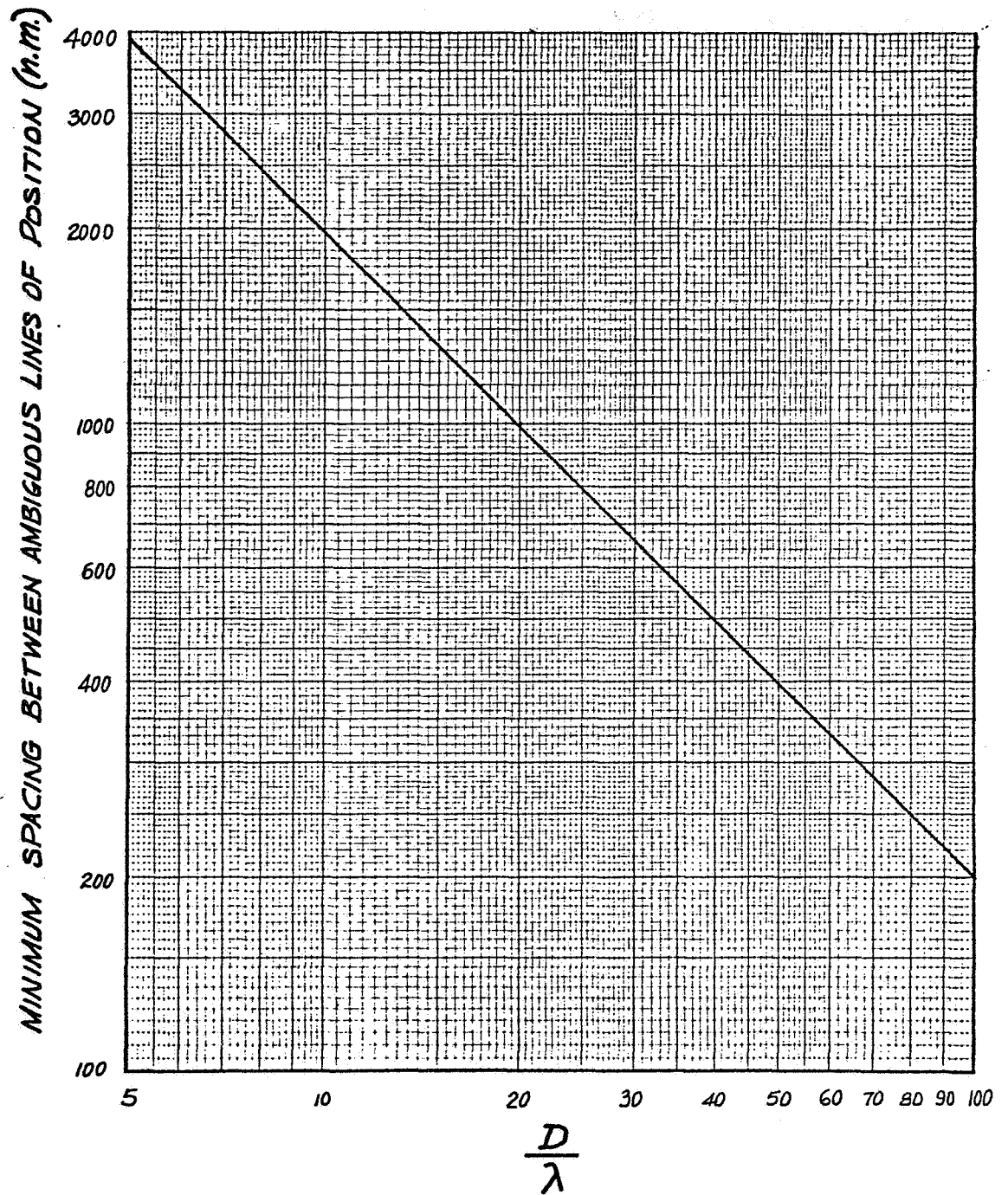
FIGURE 2 — MINIMUM SPACING BETWEEN AMBIGUOUS LINES OF POSITION ON THE SURFACE OF THE EARTH vs NUMBER OF WAVELENGTHS IN THE BASELINE OF A SYNCHRONOUS SATELLITE INTERFEROMETER

ing the phase measurements, and measuring the requir-
ed position and orientation of the satellite are dis-
cussed elsewhere.[14] It is the purpose of this work
to propose a means of reducing the multipath error
encountered in the all important phase measurement
introduced above.

2.2   The Occurrence of Multipath in the System

In general, extraneous propagation paths may
occur due to reflection from the earth's surface,
partial reflection from atmospheric sheets or
elevated layers,[15] or reflection from the user craft
or satellite parts. Earth surface reflections will
almost always occur. Partial reflection due to the
propagation medium is expected to be a rare circum-
stance most likely occurring for low satellite elev-
ation angles if at all. The case of reflection from
structures supporting the antennas is a consideration
in the design of the satellite and the positioning of
the user antenna. It should not prove difficult to
keep the satellite proper behind the patterns of
directional interferometer antennas especially in
the case of a synchronous satellite where beamwidths
of only $18°$ are required for coverage of the full
field of view on the earth. In the case of relatively

broad-beam antennas considered necessary for low
cost aircraft installations, proper antenna place-
ment may be a difficult problem but one which is
mitigated by the fact that the application of the
error reduction scheme of section 3 does not depend
upon the source of unwanted reflections. Hence all
three multipath mechanisms are handled by the pro-
cessing described in section 3.

The multipath propagation geometry due to re-
flection from the surface of the earth is shown
schematically in Figure 3. The multipath signals may
be specular or diffuse depending upon the combination
of the signal wavelength, the angle of incidence,
and the roughness of the reflecting surface. The
specular - diffuse distinction can be made using
the Rayleigh criterion:[16]

$$\Delta h \, \sin \gamma < \frac{\lambda}{8} \qquad\qquad (3)$$

where Δh is the standard deviation of the heights
of the irregularities of the scattering surface, γ
is the radiation grazing angle of incidence, and λ
is the incident radiation wavelength; when (3) holds,
specular reflection is expected. The Rayleigh crit-
erion is conveniently displayed in Figure 4, a plot
of equation (3).

SATELLITE
INTERFEROMETER

DIRECT
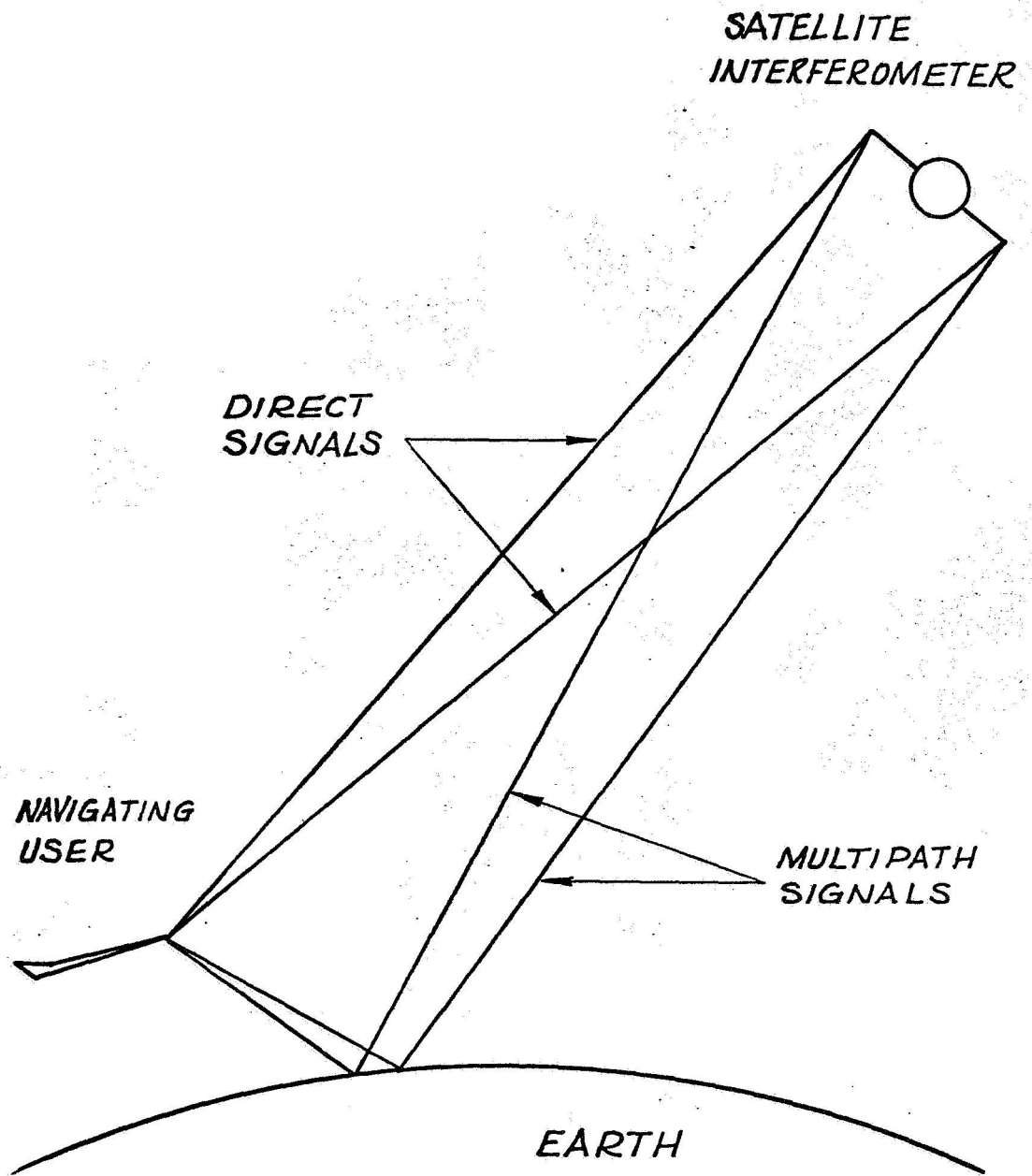SIGNALS

NAVIGATING
USER

MULTIPATH
SIGNALS

EARTH

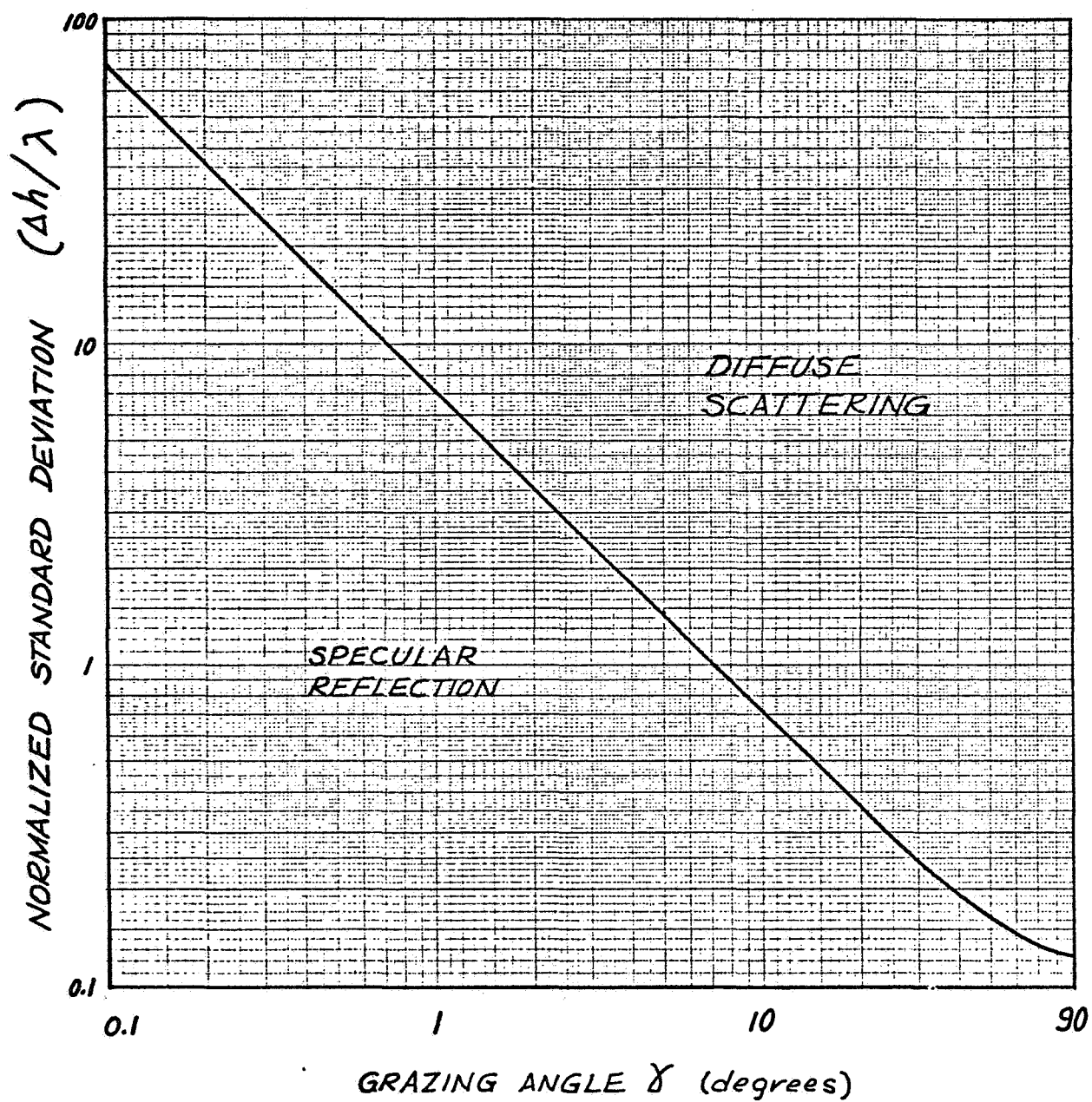FIGURE 3 — MULTIPATH PROPAGATION
GEOMETRY

FIGURE 4 - CRITERION FOR DETERMINING THE
PREDOMINANT TYPE OF SCATTERING
FROM A ROUGH SURFACE

The reflected signal voltage B can be related to the direct signal voltage A through the multipath reflection coefficient k defined by

$$B = kA$$

Neglecting atmospheric effects, A remains constant but B can be a function of time in accordance with the nature of the reflection mechanism.[17] This mechanism is embodied in k along with a factor to include any multipath suppression due to system antenna patterns. In terms of its constituent parameters,

$$k = \Gamma R P$$

where Γ is the multipath voltage amplitude suppression factor due to surface losses, R is the multipath voltage amplitude suppression factor due to surface scattering, and P is the multipath voltage amplitude suppression factor due to the system antenna patterns.

For the specularly reflected energy the factor Γ becomes the Fresnel reflection coefficient if the curvature of the earth is neglected - a good approximation for source elevation angles greater than about one degree.[18] Sherwood and Ginzton have

made measurements on homogeneous sample regions at
10 cm to determine the reflection coefficient of
several types of land and both fresh and salt water.[19]
In a world-wide navigation system, over-ocean flights
will occur most often and this last case of salt
water measurement is of particular interest. Its
results compare favorably with more recent work
done by a group at the M.I.T. Lincoln Laboratory.[20]
The M.I.T. measurements were made at UHF on signals
from the Lincoln Experimental Satellite LES-3. These
signals were received by an over-ocean aircraft and
the results are shown in Figure 5 where the multipath
suppression factor is plotted against grazing angle.
Note that at higher grazing angles the suppression
factor is smaller than that predicted by the theor-
etical specular reflection curves. This is attributed
to the presence of some diffuse scattering.

Scattering arises from surface irregularities.
For a surface which is only slightly rough, specular
reflection can be said to occur in which case R is
given as a function of the surface roughness parameter
$(\Delta h \sin \gamma / \lambda)$ by Figure 6.[18] For very rough surfaces
$(\Delta h \gg \lambda)$ and other than extremely shallow incidence
angles, diffuse scattering occurs. In this case R is
independent of the grazing angle of incidence, the

FIGURE 5 — MULTIPATH VOLTAGE AMPLITUDE
SUPPRESSION FACTOR (Γ) FOR
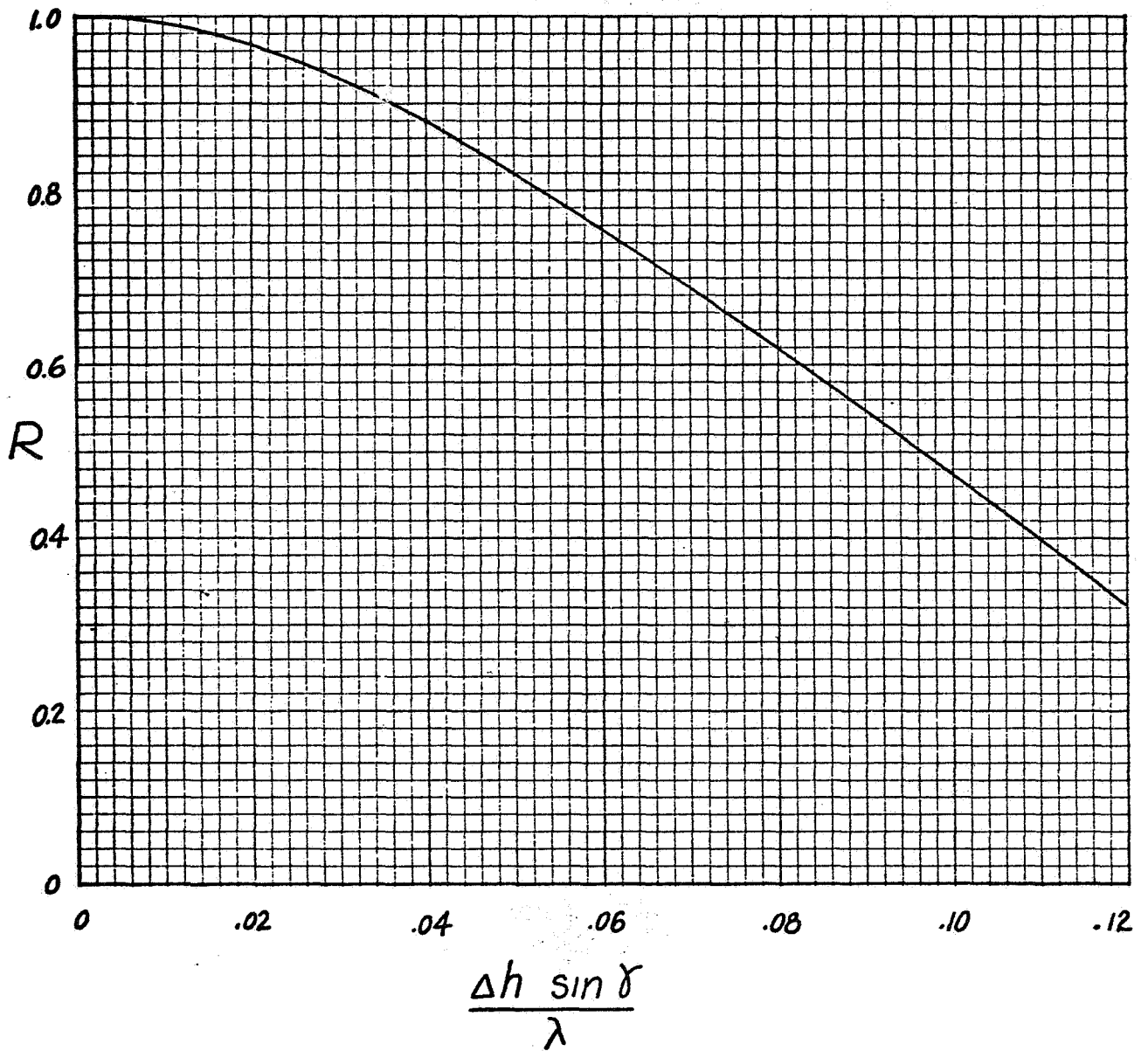SEA WATER vs GRAZING ANGLE
(after reference 20)
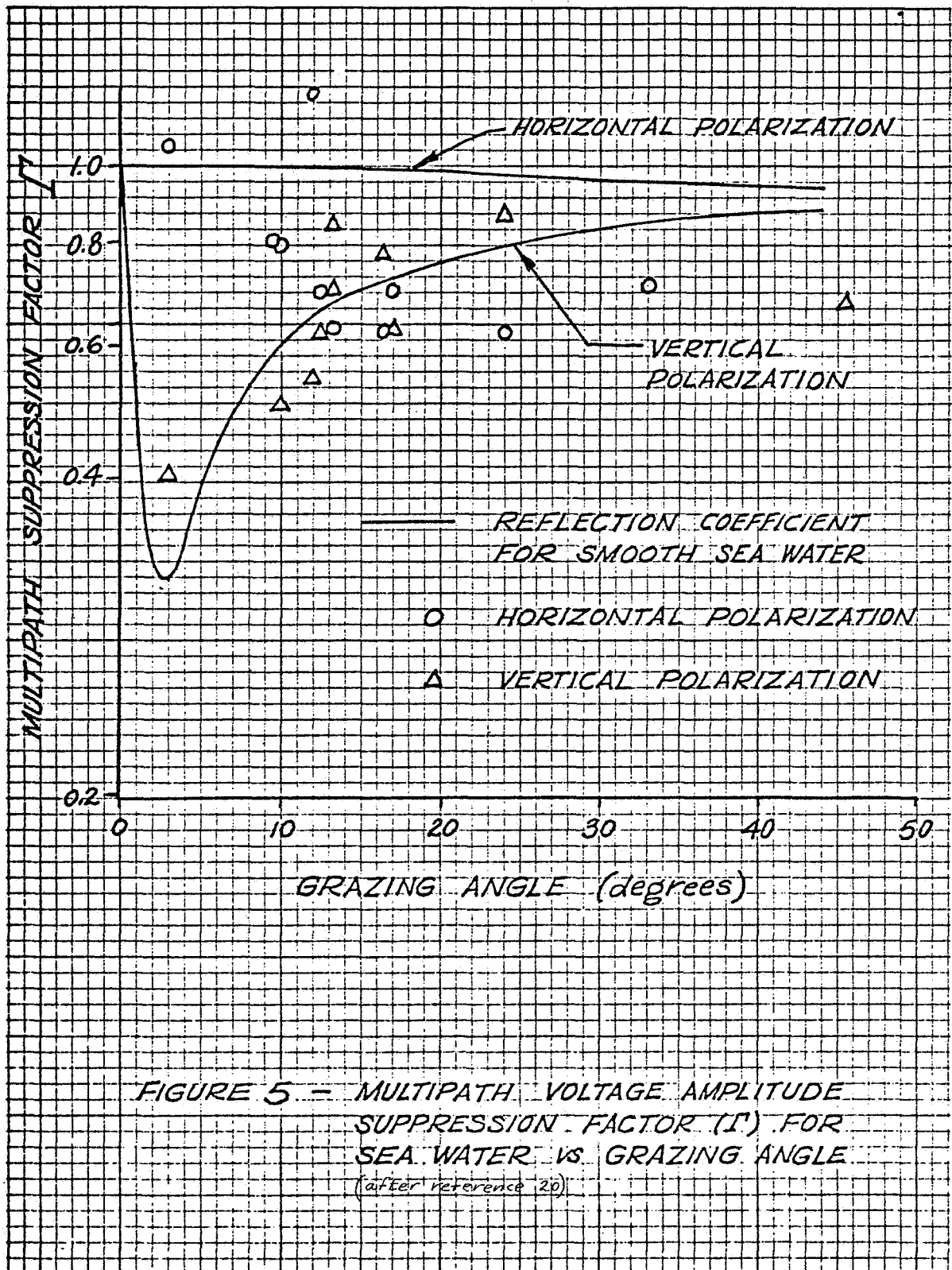
FIGURE 6 - MULTIPATH VOLTAGE AMPLITUDE
SUPPRESSION FACTOR R DUE
TO SPECULAR SCATTERING AS
A FUNCTION OF THE SURFACE
ROUGHNESS PARAMETER $\frac{\Delta h \sin \gamma}{\lambda}$
(after reference 18)

surface deviation, and the wavelength. McGavin and Maloney,[21] measuring at 1046 MHz, have determined a mean diffuse case value of 0.35 for R with standard deviation 0.15.

The factor P, which can serve to further reduce the multipath reflection coefficient, arises from the use of other than omnidirectional antennas. For example, the typical cardioid main-lobe pattern shown on an aircraft in Figure 7 places the earth-reflected multipath in a reduced gain position. The figure applies to the case where the satellite is very far away so that the reflection incidence angle approximately equals the satellite elevation angle at the aircraft. Let the gain of the antenna be given by $G(\eta)$ where η is measured from a line perpendicular to the top of the aircraft fuselage. It follows that

$$P = \frac{G(\eta + 2\gamma)}{G(\eta)}$$

It is possible to approximate most antenna patterns over the 2γ angle of interest by a constant rate of decrease in gain given here in decibels per degree. Assuming a gain of unity in the direction of the direct signal path, Figure 8 relates P to the satellite elevation angle γ for patterns decreasing

USER ANTENNA
PATTERN

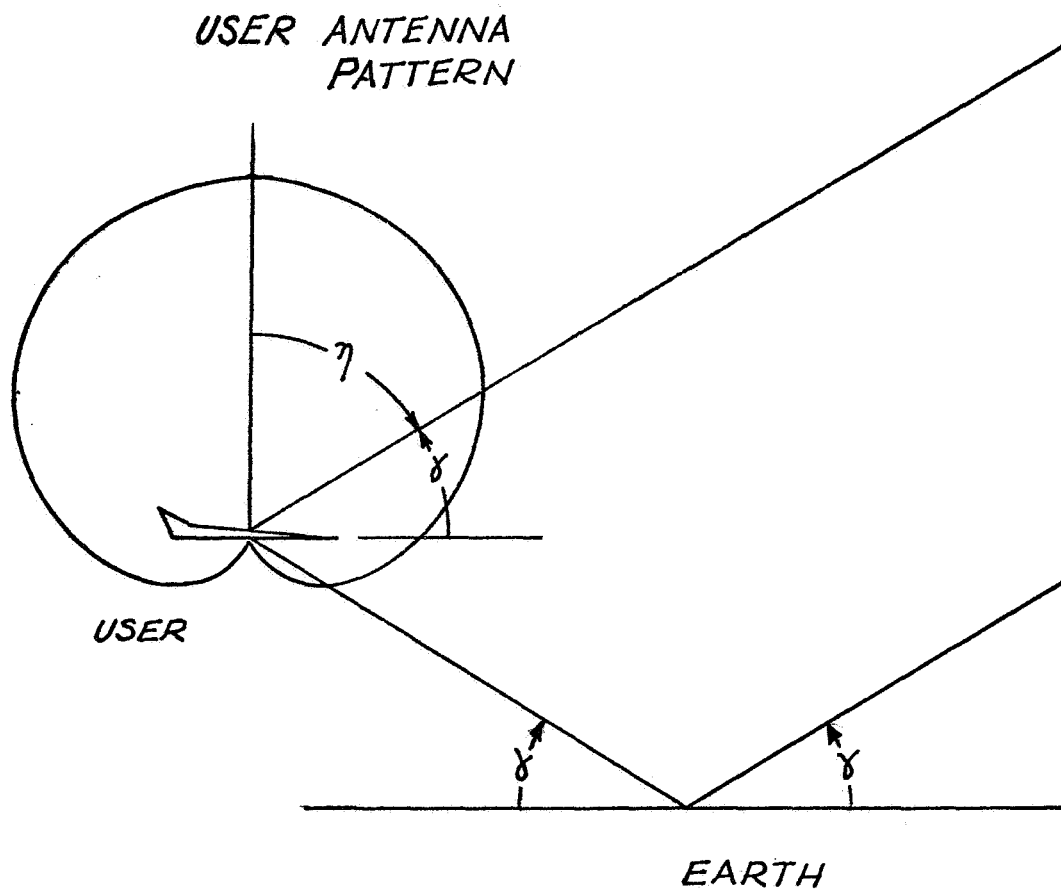η

γ

USER

γ

γ

EARTH

FIGURE 7 — GEOMETRY DEFINING THE MULTIPATH
AMPLITUDE SUPPRESSION FACTOR
DUE TO THE USER ANTENNA PATTERN
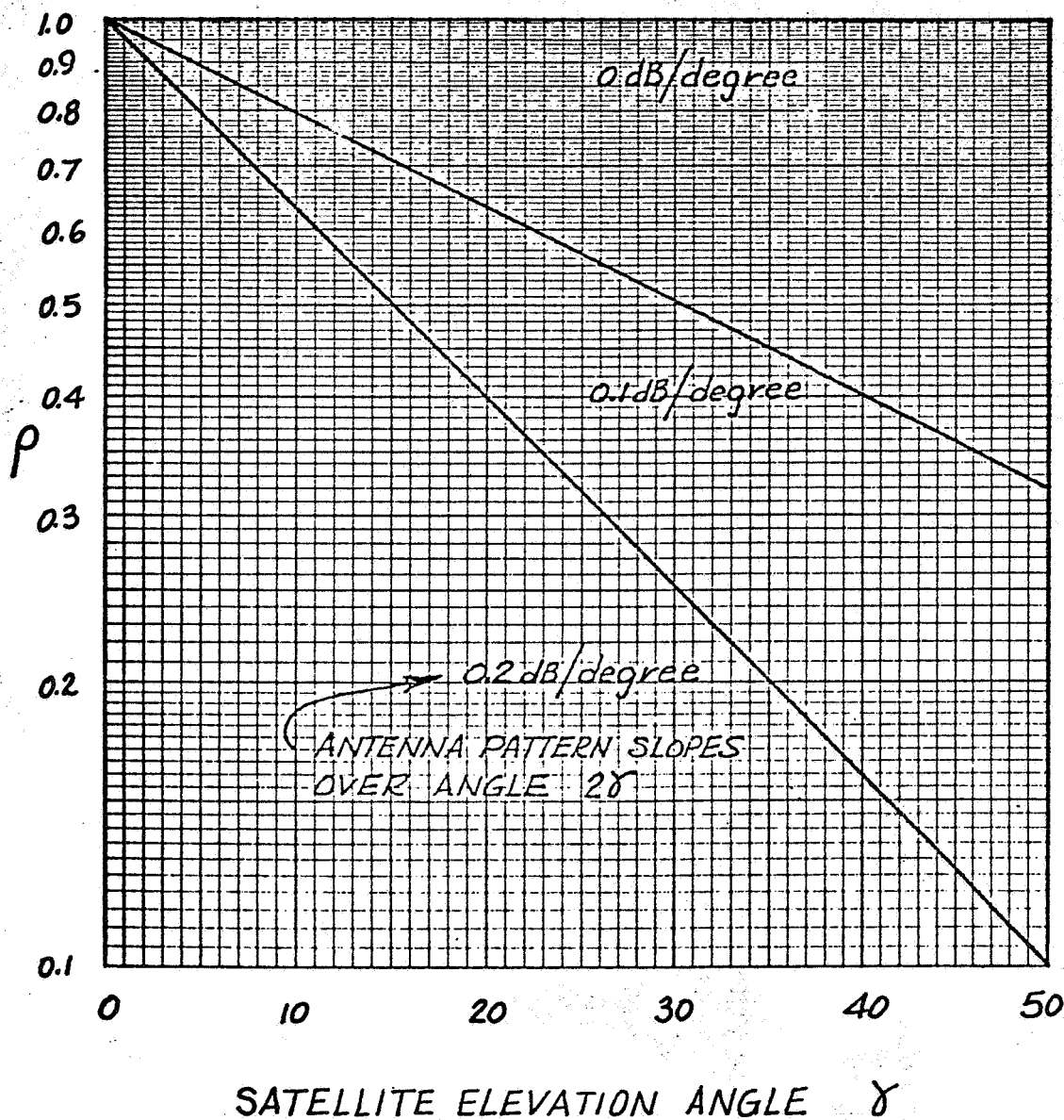
FIGURE 8 — MULTIPATH VOLTAGE AMPLITUDE SUPPRESSION FACTOR ρ DUE TO THE NAVIGATING USER'S ANTENNA PATTERN CHARACTERIZED BY ITS ATTENUATION PER DEGREE

by 0.1 and 0.2 decibels per degree. In theory ρ would
be the product of the suppression factors of both the
user and satellite antennas. However, at a high alt-
itude interferometer satellite, the direct and multi-
path signals will be too close together to result in
a suppression factor at the satellite which is sig-
nificantly different from unity.

3.0   EXPRESSING THE SYSTEM PHASE-MEASUREMENT ERROR

Positional information is obtained from the phase difference between the signals at the spaced antennas of the satellite interferometer (in accordance with equation (I)). The phase difference between multipath contaminated signals will in general differ from that uncontaminated difference which yields a user's true angular position.   For the purpose of this derivation, it is convenient to represent the system's constituent signals as phasors. This is done in Figure 9 where

A_i = magnitude of direct signal i

B_i = magnitude of multipath signal i

C_i = magnitude of resultant signal i

α_i = phase angle of direct signal i

β_i = phase angle of multipath signal i

α_i' = phase angle of resultant signal i

i = 1, 2

From Figure 9,

$$\left(\alpha_2' - \alpha_1'\right) = \left(\alpha_2 - \alpha_1\right) + \beta_2 - \beta_1 + \delta_1 - \delta_2$$

$$= \left(\alpha_2 - \alpha_1\right) + \left(\gamma_2 - \gamma_1\right)$$
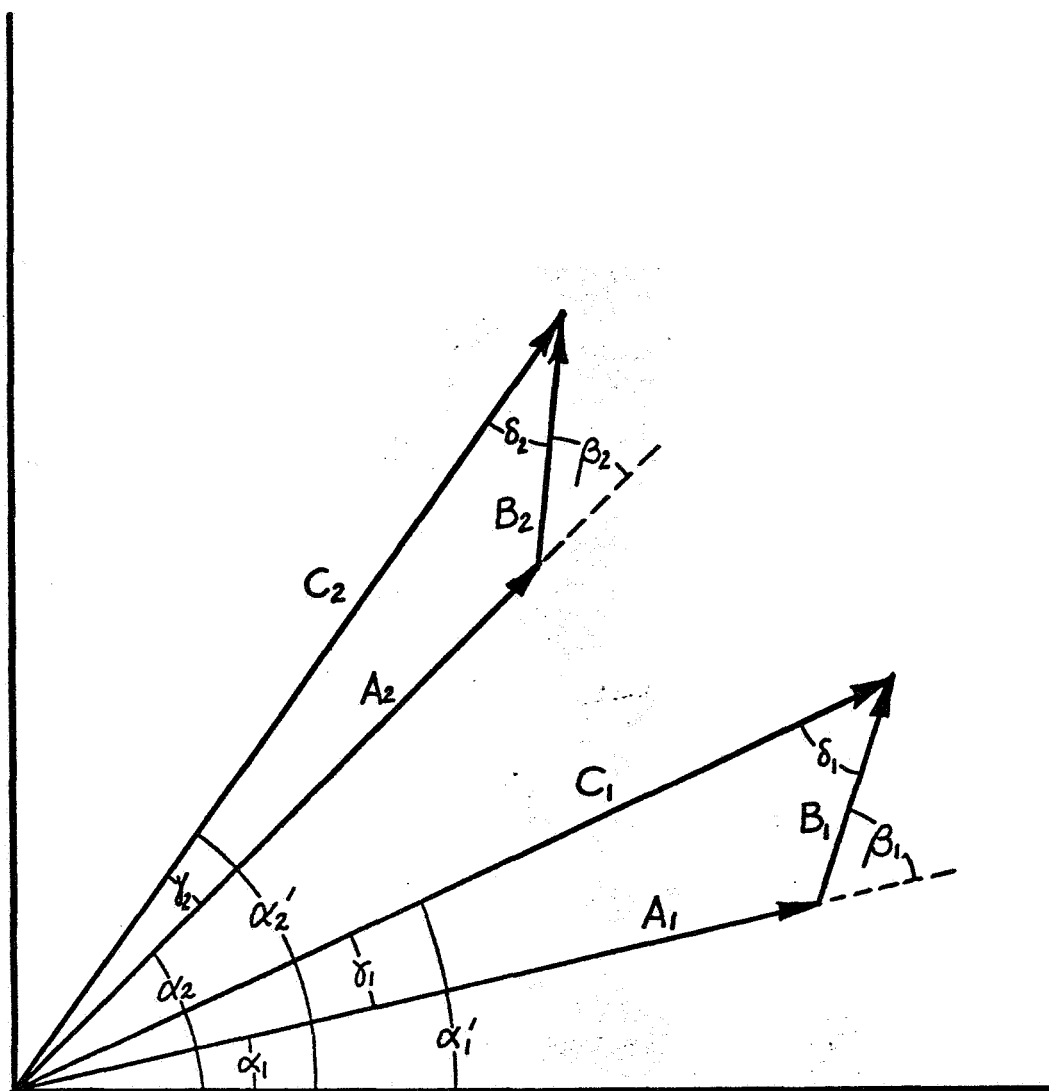
FIGURE 9 — PHASOR DIAGRAM FOR MULTIPATH CONTAMINATED SIGNALS AT THE SATELLITE INTERFEROMETER

or

$$\Delta \alpha' = \Delta \alpha + \epsilon \qquad (3)$$

where

$\Delta \alpha' = (\alpha_2' - \alpha_1')$, the measured phase difference

$\Delta \alpha = (\alpha_2 - \alpha_1)$, the desired phase difference

$\epsilon = (\gamma_2 - \gamma_1)$, the error due to multipath

In terms of direct and multipath signal amplitudes and multipath signal phases, ϵ becomes

$$\epsilon = \tan^{-1} \frac{B_2 \sin \beta_2}{A_2 + B_2 \cos \beta_2} - \tan^{-1} \frac{B_1 \sin \beta_1}{A_1 + B_1 \cos \beta_1}$$

Hence

$$\Delta \alpha' = \Delta \alpha + \tan^{-1} \frac{B_2 \sin \beta_2}{A_2 + B_2 \cos \beta_2} - \tan^{-1} \frac{B_1 \sin \beta_1}{A_1 + B_1 \cos \beta_1} \qquad (4)$$

The interferometer baseline is not likely to be so large that direct rays propagating to its spaced antennas will undergo significantly different attenuation. Moreover the two multipath signals are likely to have specular reflection points close enough together to insure equal reflection coefficients for

virtually all cases. These conditions are incorporated in succeeding calculations by letting $A_1 = A_2 = A$ and $B_1 = B_2 = B$.

The difference of two arctangent functions appearing in equation (4) can be written as a single arctangent function plus a constant according to the following identity

$$tan^{-1}(x) - tan^{-1}(Y) = tan^{-1}\left(\frac{X-Y}{1+XY}\right) + K \qquad (5)$$

where

$$K = \begin{cases} 0 & XY > -1 \\ \pi & X > 0, \ XY < -1 \\ -\pi & X < 0, \ XY < -1 \end{cases}$$

$$X = \frac{B \sin \beta_2}{A + B \cos \beta_2}$$

$$Y = \frac{B \sin \beta_1}{A + B \cos \beta_1}$$

Using equation (5) in equation (4) ,

$$\Delta\alpha' = \Delta\alpha + tan^{-1}\left[\frac{AB(\sin\beta_2 - \sin\beta_1) + B^2\sin(\beta_2 - \beta_1)}{A^2 + AB(\cos\beta_1 + \cos\beta_2) + B^2\cos(\beta_2 - \beta_1)}\right] + K \qquad (6)$$

If the multipath phase angles are equal, the measured phase difference will equal the desired phase difference without error. That is to say, when $\beta_1 = \beta_2$, then $\Delta\alpha' = \Delta\alpha$ which requires that $K = 0$.

It will be assumed that $B/A \ll 1$. This effectively says that the factors comprising the multipath reflection coefficient (k) have substantial effect. Under this assumption, equation (6) becomes

$$\Delta\alpha' = \Delta\alpha + \frac{B}{A}\left(\sin\beta_2 - \sin\beta_1\right) \tag{7}$$

At a wavelength λ, the change in phase over path length ℓ (in free space) is given by $\frac{2\pi\ell}{\lambda}$. Suppose the direct paths to the first and second satellite interferometer antennas are given by ℓ_1 and ℓ_2 respectively. Let the total reflected signal paths be designated by ℓ_3 and ℓ_4 where ℓ_3 is associated with the first satellite antenna and ℓ_4 is associated with the second. The path length differences between the direct and reflected signal paths are then $\ell_3 - \ell_1$ for the first antenna and $\ell_4 - \ell_2$ for the second. It follows that

$$\beta_1 = \frac{2\pi(\ell_3 - \ell_1)}{\lambda}$$

and $\qquad \beta_2 = \dfrac{2\pi\,(\ell_4 - \ell_2)}{\lambda}$

Equation (7) becomes

$$\Delta\alpha' = \Delta\alpha + \frac{B}{A}\left\{ \sin \frac{2\pi(\ell_4 - \ell_2)}{\lambda} - \sin \frac{2\pi(\ell_3 - \ell_1)}{\lambda} \right\} \qquad (8)$$

where the second term of (8) is the phase error due to multipath propagation.

4.0 SIGNAL-DESIGN ERROR REDUCTION

Equation (8) shows the multipath phase error and its dependence on operating wavelength and system geometry. By allowing either of these parameters to vary with time, the phase measurement will take on a time variation. It is proposed to have the navigation receiver low-pass filter such a time-varying phase measurement to extract an average value containing a reduced error component.

4.1 FREQUENCY-SWEEP TECHNIQUE

4.1.1 Processing the Phase Measurement

In the frequency-sweep technique, the otherwise continuous wave navigation signal is swept in frequency at the transmitter. To investigate the effect of the frequency sweeping, the path lengths are considered fixed while the wavelength λ is made to vary with time. Hence the phase error ϵ due to multipath propagation becomes

$$\epsilon(t) = \frac{B}{A} \left\{ \sin \frac{L_1}{\lambda(t)} - \sin \frac{L_2}{\lambda(t)} \right\} \qquad (9)$$

where $L_1 = 2\pi (\ell_4 - \ell_2)$

$L_2 = 2\pi (\ell_3 - \ell_1)$

Choose a sinusoidal frequency sweep about center frequency f_o by letting $f(t) = f_o (1 + q \cos pt)$ where q is the sweep width factor and p is the sweep frequency.
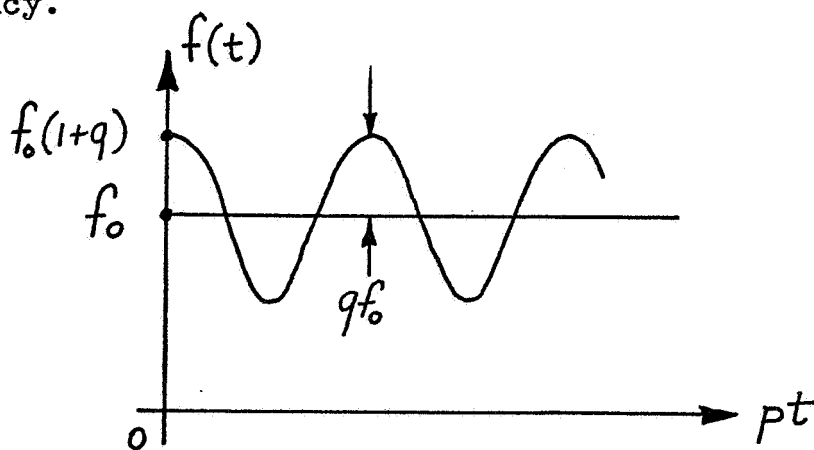

FIGURE 10 – FREQUENCY SWEEP OF TRANSMITTED SIGNAL

Now

$$\epsilon(t) = \frac{B}{A} \left\{ \sin \frac{L_1 f(t)}{C} - \sin \frac{L_2 f(t)}{C} \right\}$$

$$= \frac{B}{A} \left\{ \sin \frac{L_1 f_o (1 + q \cos pt)}{C} - \sin \frac{L_2 f_o (1 + q \cos pt)}{C} \right\} \qquad (10)$$

where C is the velocity of propagation assuming a
free space path.

Expanding (10),

$$E(t) = \frac{B}{A}\left[\sin\left(\frac{L_1 f_0}{C}\right)\cos\left(\frac{L_1 f_0 q \cos pt}{C}\right) + \cos\left(\frac{L_1 f_0}{C}\right)\sin\left(\frac{L_1 f_0 q \cos pt}{C}\right)\right.$$

$$\left. - \sin\left(\frac{L_2 f_0}{C}\right)\cos\left(\frac{L_2 f_0 q \cos pt}{C}\right) - \cos\left(\frac{L_2 f_0}{C}\right)\sin\left(\frac{L_2 f_0 q \cos pt}{C}\right)\right]$$

But

$$\cos\left(\frac{L_i f_0 q \cos pt}{C}\right) = J_0\left(\frac{L_i f_0 q}{C}\right) - 2\left[J_2\left(\frac{L_i f_0 q}{C}\right)\cos 2pt - J_4\left(\frac{L_i f_0 q}{C}\right)\cos 4pt + \cdots\right]$$

and
$$i = 1,2$$

$$\sin\left(\frac{L_i f_0 q \cos pt}{C}\right) = 2\left[J_1\left(\frac{L_i f_0 q}{C}\right)\cos pt - J_3\left(\frac{L_i f_0 q}{C}\right)\cos 3pt + \cdots\right]$$

$$i = 1,2$$

Let $\frac{L_1 f_0}{C} = a$ and $\frac{L_2 f_0}{C} = b$ to write

$$E(t) = \frac{B}{A}\left\{\left[J_0(qa) + 2\sum_{k=1}^{\infty}(-1)^k J_{2k}(qa)\cos 2kpt\right]\sin a\right.$$

$$+ \left[2\sum_{k=0}^{\infty}(-1)^k J_{2k+1}(qa)\cos(2k+1)pt\right]\cos a$$

$$- \left[J_0(qb) + 2\sum_{k=1}^{\infty}(-1)^k J_{2k}(qb)\cos 2kpt\right]\sin b$$

$$\left. - \left[2\sum_{k=0}^{\infty}(-1)^k J_{2k+1}(qb)\cos(2k+1)pt\right]\cos b\right\} \qquad (11)$$

Varying λ with time makes all quantities of equation (3) time varying:

$$\Delta\alpha'(t) = \Delta\alpha(t) + \epsilon(t)$$

$$= \frac{2\pi(\ell_2-\ell_1)f(t)}{C} + \epsilon(t)$$

$$= \frac{2\pi(\ell_2-\ell_1)f_o}{C} + \frac{2\pi(\ell_2-\ell_1)f_o\,q\cos pt}{C}$$

$$+ \frac{B}{A}\left\{\left[J_o(qa) + 2\sum_{k=1}^{\infty}(-1)^k J_{2k}(qa)\cos 2kpt\right]\sin a\right.$$

$$+\left[2\sum_{k=0}^{\infty}(-1)^k J_{2k+1}(qa)\cos(2k+1)pt\right]\cos a$$

$$-\left[J_o(qb) + 2\sum_{k=1}^{\infty}(-1)^k J_{2k}(qb)\cos 2kpt\right]\sin b$$

$$\left.\left[2\sum_{k=0}^{\infty}(-1)^k J_{2k+1}(qb)\cos(2k+1)pt\right]\cos b\right\} \quad (12)$$

The navigation receiver will low-pass filter (12) to obtain

$$\Delta\alpha'_{LP} = \frac{2\pi(\ell_2-\ell_1)f_o}{C} + \frac{B}{A}\left[J_o(qa)\sin a - J_o(qb)\sin b\right] \quad (13)$$

Note that the desired phase measurement $\Delta\alpha$ appears as the first term of equation (13). The second term of (13) is the new, generally smaller error contribution. In filtering (12) to obtain (13), it is assumed that

$$\frac{1}{T}\int_{0}^{T} \cos pt\, dt = \frac{\sin pT}{pT} \to 0$$

For practical purposes this is true when $T \gg \frac{1}{p}$ where T is the integration time. Again, practically speaking, navigation measurements should be made as quickly as possible. Arbitrarily assuming a maximum allowable integration time of one second will permit the calculation of a minimum sweep rate. With $T = 1$, $\frac{\sin p}{p}$ will approach zero to within 10^{-5} for $p = 10^5$ sec^{-1} corresponding to an estimated sweep frequency of 16 KHz.

4.1.2   The Effect of the Sweep Width Factor

Equation (13) shows that the magnitude of the final error depends upon the sweep width factor q. The term of interest is the processed error ϵ_{LP} given by

$$\epsilon_{LP} = \frac{B}{A}\left[J_o(qa)\sin a - J_o(qb)\sin b \right] \qquad (14)$$

where

$$a = \frac{L_1 f_o}{c} = \frac{2\pi f_o}{c}(\ell_4 - \ell_2) \qquad (15a)$$

$$b = \frac{L_2 f_o}{c} = \frac{2\pi f_o}{c}(\ell_3 - \ell_1) \qquad (15b)$$

In terms of multipath over direct path propagation delay time τ, either path length difference in (15) can be bounded as follows

$$c\tau_{min} < \begin{matrix} (\ell_4 - \ell_2) \\ OR \\ (\ell_3 - \ell_1) \end{matrix} < c\tau_{max} \qquad (16)$$

where τ_{min} and τ_{max} are a user's minimum and maximum time delay differences. Assuming the satellite is far enough away so that all propagation paths from the earth to the satellite are parallel and neglecting the earth's curvature, τ is given by (derived on the basis of Figure 11)

$$\tau = \frac{h(1 - \cos 2\gamma)}{c \sin \gamma} \qquad (17)$$

where h is the user's altitude and γ is the elevation angle of the satellite. Equation (17) is shown in Figure 12.

TO ONE
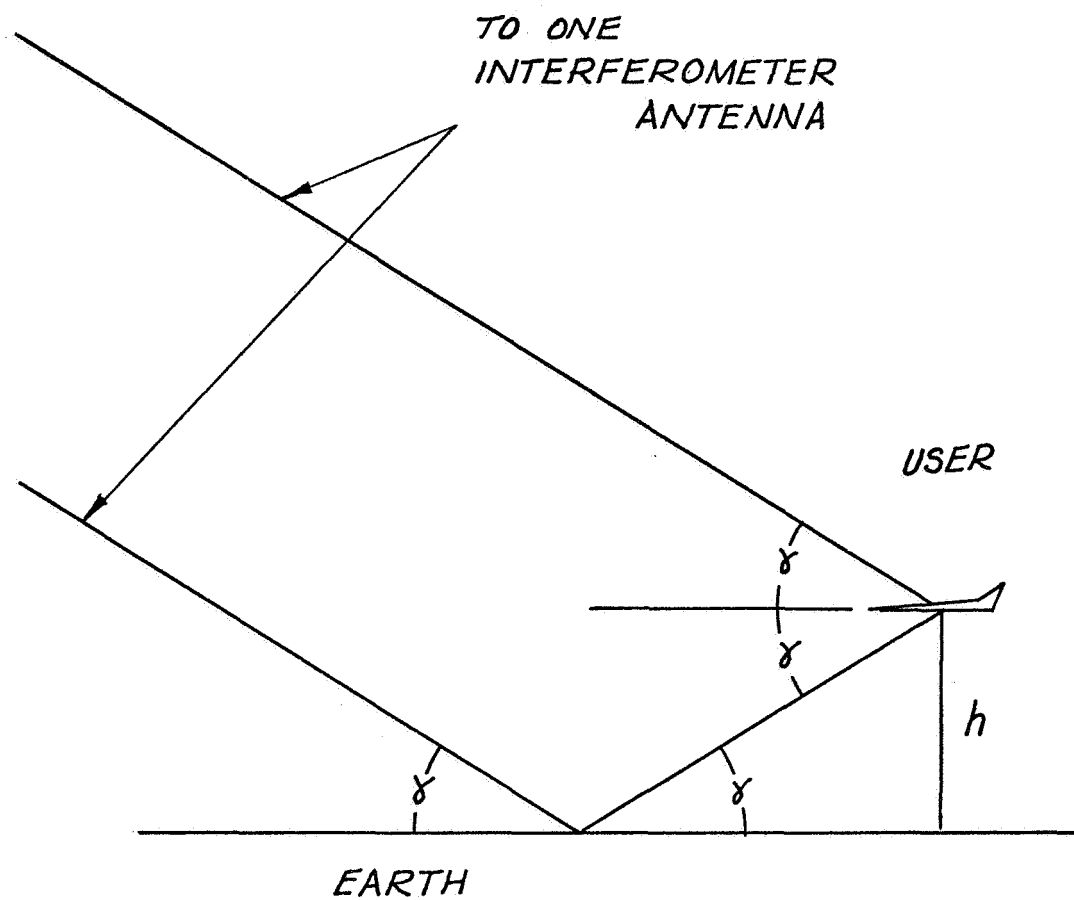INTERFEROMETER
ANTENNA

USER

γ

γ

h

γ

γ

EARTH

FIGURE 11 — GEOMETRY USED TO DERIVE
TIME DELAY DIFFERENCE τ

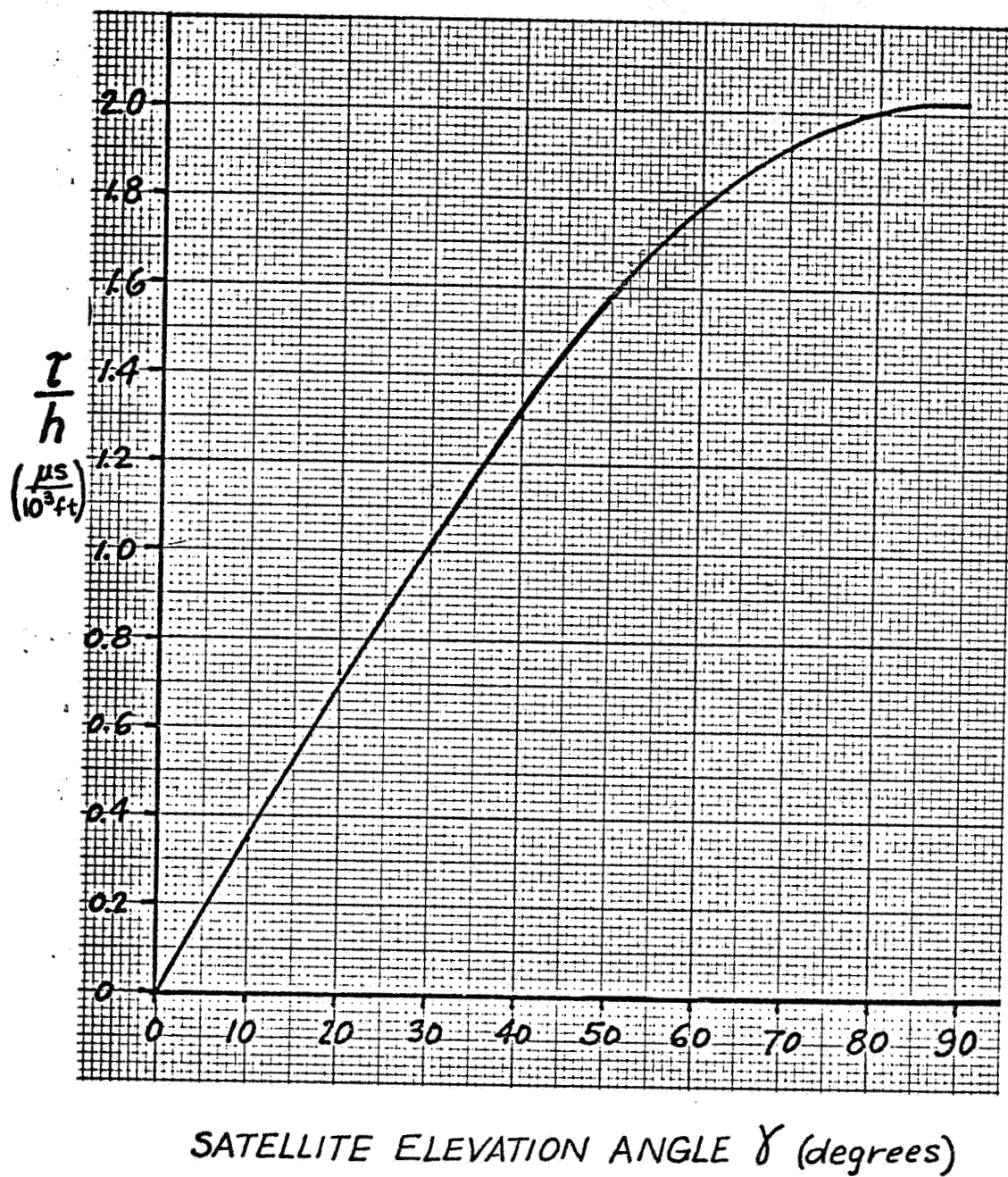SATELLITE ELEVATION ANGLE γ (degrees)

FIGURE 12 — NORMALIZED RELATIVE MULTIPATH DELAY TIME

In general $(\ell_4 - \ell_2)$ does not equal $(\ell_3 - \ell_1)$. If one of these differences is assigned a value in the range of (16), it remains to determine the close but generally different value of the other difference. To do this, let

$$\mathcal{L}_2 = \mathcal{L}_1 + \Delta \mathcal{L} \tag{18}$$

where
$$\mathcal{L}_1 = \ell_4 - \ell_2$$
$$\mathcal{L}_2 = \ell_3 - \ell_1$$

and $\Delta \mathcal{L}$ is small compared to either $\mathcal{L}_1$ or $\mathcal{L}_2$ in accordance with the geometry of the system.

Recalling that the $\mathcal{L}_i$ ($i = 1, 2$) are related to their respective relative delay times τ_i through the velocity of propagation C, either of them can be expressed as an explicit function of γ. This will be done with $\ell_4 - \ell_2$:

$$\ell_4 - \ell_2 = c\tau = \frac{h(1 - \cos 2\gamma)}{\sin \gamma} = f(\gamma)$$

For any particular elevation angle, say γ_1 ,

$$\ell_4 - \ell_2 = f(\gamma_1)$$

It follows then that

$$\ell_3 - \ell_1 = f(\gamma_1 + \Delta\gamma)$$

where $\Delta\gamma$ is a small elevation angle increment phys-
ically associated with the angular separation of the
interferometer antennas. Expanding $\ell_3 - \ell_1$ about γ_1,

$$\ell_3 - \ell_1 \cong f(\gamma_1) + \Delta\gamma f'(\gamma_1)$$

$$= \ell_4 - \ell_2 + 2h(\Delta\gamma)\cos\gamma_1$$

Since this result is true for any elevation angle, γ_1
may be replaced by γ to obtain

$$\Delta\mathscr{L} = 2h(\Delta\gamma)\cos\gamma$$

as shown in Figure 13. With the notation of (18) and
noting that the maximum value of the error ϵ_{max} is
$2\frac{B}{A}$, the normalized phase error becomes

$$\frac{\epsilon_{LP}}{\epsilon_{max}} = \frac{1}{2}\left\{ J_0\left(\frac{2\pi f_0}{c} q\mathscr{L}_1\right) \sin\left(\frac{2\pi f_0}{c}\mathscr{L}_1\right)\right.$$

$$\left. - J_0\left[\frac{2\pi f_0}{c} q(\mathscr{L}_1 + \Delta\mathscr{L})\right] \sin\left[\frac{2\pi f_0}{c}(\mathscr{L}_1 + \Delta\mathscr{L})\right] \right\}$$

$$\frac{|\alpha_1 - \alpha_2|}{h(\Delta\gamma)}$$

SATELLITE ELEVATION ANGLE γ (degrees)

FIGURE 13 — NORMALIZED DIFFERENCE IN
PATH LENGTH DIFFERENCES

Expanding,

$$\frac{\epsilon_{LP}}{\epsilon_{max}} = \frac{1}{2}\left\{ J_o\left(\frac{2\pi f_o}{c} q\alpha_1\right) \sin\left(\frac{2\pi f_o}{c}\alpha_1\right) \right.$$

$$- J_o\left[\frac{2\pi f_o}{c} q(\alpha_1 + \Delta\alpha)\right]\left[\sin\left(\frac{2\pi f_o}{c}\alpha_1\right)\cos\left(\frac{2\pi f_o}{c}\Delta\alpha\right)\right.$$

$$\left.\left.+ \cos\left(\frac{2\pi f_o}{c}\alpha_1\right)\sin\left(\frac{2\pi f_o}{c}\Delta\alpha\right)\right]\right\} \quad (19)$$

For f_o up to about 10 GHz,

$$\frac{\epsilon_{LP}}{\epsilon_{max}} = \frac{1}{2}\left\{ J_o\left(\frac{2\pi f_o}{c} q\alpha_1\right) \sin\left(\frac{2\pi f_o}{c}\alpha_1\right) \right.$$

$$- J_o\left[\frac{2\pi f_o}{c} q(\alpha_1 + \Delta\alpha)\right]\left[\sin\left(\frac{2\pi f_o}{c}\alpha_1\right)\right.$$

$$\left.\left.+ \frac{2\pi f_o}{c}(\Delta\alpha)\cos\left(\frac{2\pi f_o}{c}\alpha_1\right)\right]\right\} \quad (20)$$

in which

$$J_o\left[\frac{2\pi f_o}{c} q(\alpha_1 + \Delta\alpha)\right] = \frac{1}{\pi}\int_0^\pi \cos\left[\frac{2\pi f_o}{c} q(\alpha_1 + \Delta\alpha)\sin x\right] dx$$

$$= \frac{1}{\pi}\int_0^\pi \cos\left[\frac{2\pi f_o}{c} q\alpha_1 \sin x\right]\cos\left[\frac{2\pi f_o}{c} q(\Delta\alpha)\sin x\right] dx$$

$$- \frac{1}{\pi}\int_0^\pi \sin\left[\frac{2\pi f_o}{c} q\alpha_1 \sin x\right]\sin\left[\frac{2\pi f_o}{c} q(\Delta\alpha)\sin x\right] dx$$

$$\approx \frac{1}{\pi} \int_0^\pi \cos\left[\frac{2\pi f_0}{c} q \alpha_1 \sin x\right] dx$$

$$- \frac{1}{\pi} \int_0^\pi \left[\frac{2\pi f_0}{c} q (\Delta \alpha) \sin x\right] \sin\left[\frac{2\pi f_0}{c} q \alpha_1 \sin x\right] dx$$

$$= J_0\left(\frac{2\pi f_0}{c} q \alpha_1\right) - \frac{2\pi f_0}{c} q (\Delta \alpha) \frac{1}{\pi} \int_0^\pi \sin x \sin\left[\frac{2\pi f_0}{c} q \alpha_1 \sin x\right] dx$$

$$= J_0\left(\frac{2\pi f_0}{c} q \alpha_1\right) - \frac{2\pi f_0}{c} q (\Delta \alpha) J_1\left(\frac{2\pi f_0}{c} q \alpha_1\right) \qquad (21)$$

Using (21), equation (20) becomes

$$\frac{\epsilon_{LP}}{\epsilon_{max}} = \frac{\pi f_0}{c} (\Delta \alpha) \left[q J_1\left(\frac{2\pi f_0}{c} q \alpha_1\right) \sin\left(\frac{2\pi f_0}{c} \alpha_1\right) \right.$$

$$\left. - J_0\left(\frac{2\pi f_0}{c} q \alpha_1\right) \cos\left(\frac{2\pi f_0}{c} \alpha_1\right) \right]$$

$$= \frac{\pi f_0}{c} (\Delta \alpha) \left[q J_1\left(2\pi f_0 q \tau\right) \sin\left(2\pi f_0 \tau\right) - J_0\left(2\pi f_0 q \tau\right) \cos\left(2\pi f_0 \tau\right) \right] \qquad (22)$$

Equation (22) has been plotted with the aid of the Moore School RCA Spectra 70 computer. For the computer computation, certain parameters must be fixed. By choosing values for f_0, h, and $\Delta \gamma$, the normalized error can be plotted against the sweep width factor q with the satellite elevation angle γ

as a parameter.

The user is chosen to be a supersonic transport. From the four proposed frequency assignments, the L-band allocation will be chosen for reasons of less man-made interference and less ionospheric refraction than VHF and for reasons of more economy and less propagation attenuation than the 6 cm and 2 cm bands. The quantity $\Delta\gamma$ depends upon the interferometer baseline D and is given approximately by

$$\Delta\gamma \approx \frac{D}{S} \quad \text{radians}$$

where S is the satellite slant range ($S \approx 3.9 \times 10^7$ m for a synchronous satellite). If it is assumed that a navigator knows his position to within 1000 nautical miles, Figure 2 shows that additional ambiguity-resolving apparatus will not be needed for D up to 20λ.

From the above discussion, the following values are chosen to obtain Figure 14:

Center frequency, f_o = 1600 MHz

SST altitude, h = 2×10^4 m (65,000 feet)

Angular antenna
separation, $\Delta\gamma = \frac{20\lambda}{S} = \frac{3.75 \text{ m}}{3.9 \times 10^7 \text{ m}} \approx 10^{-7}$ radian

FIGURE 14 — NORMALIZED PHASE ERROR AS A FUNCTION OF THE SWEEP WIDTH FACTOR WITH THE SATELLITE ELEVATION ANGLE AS PARAMETER
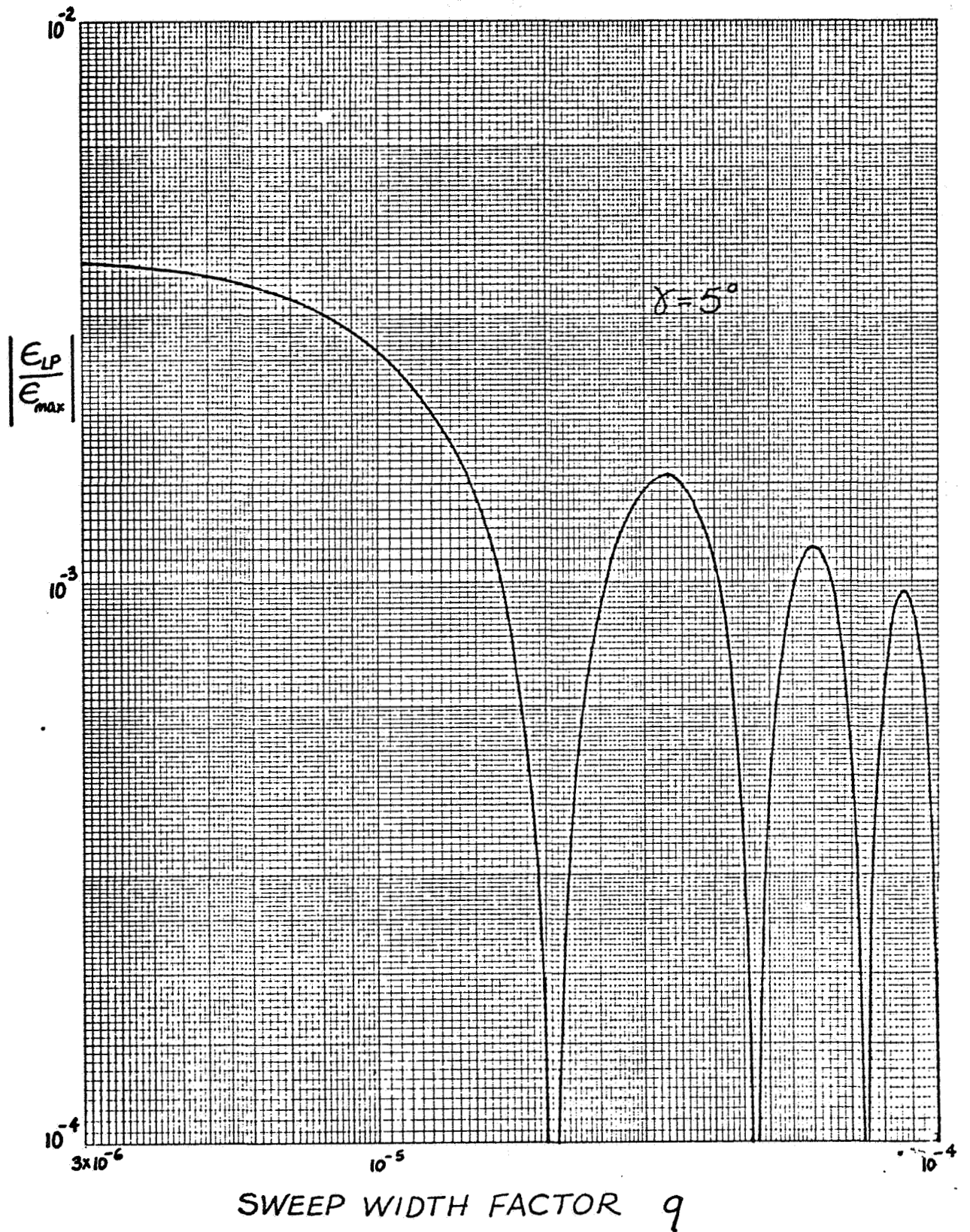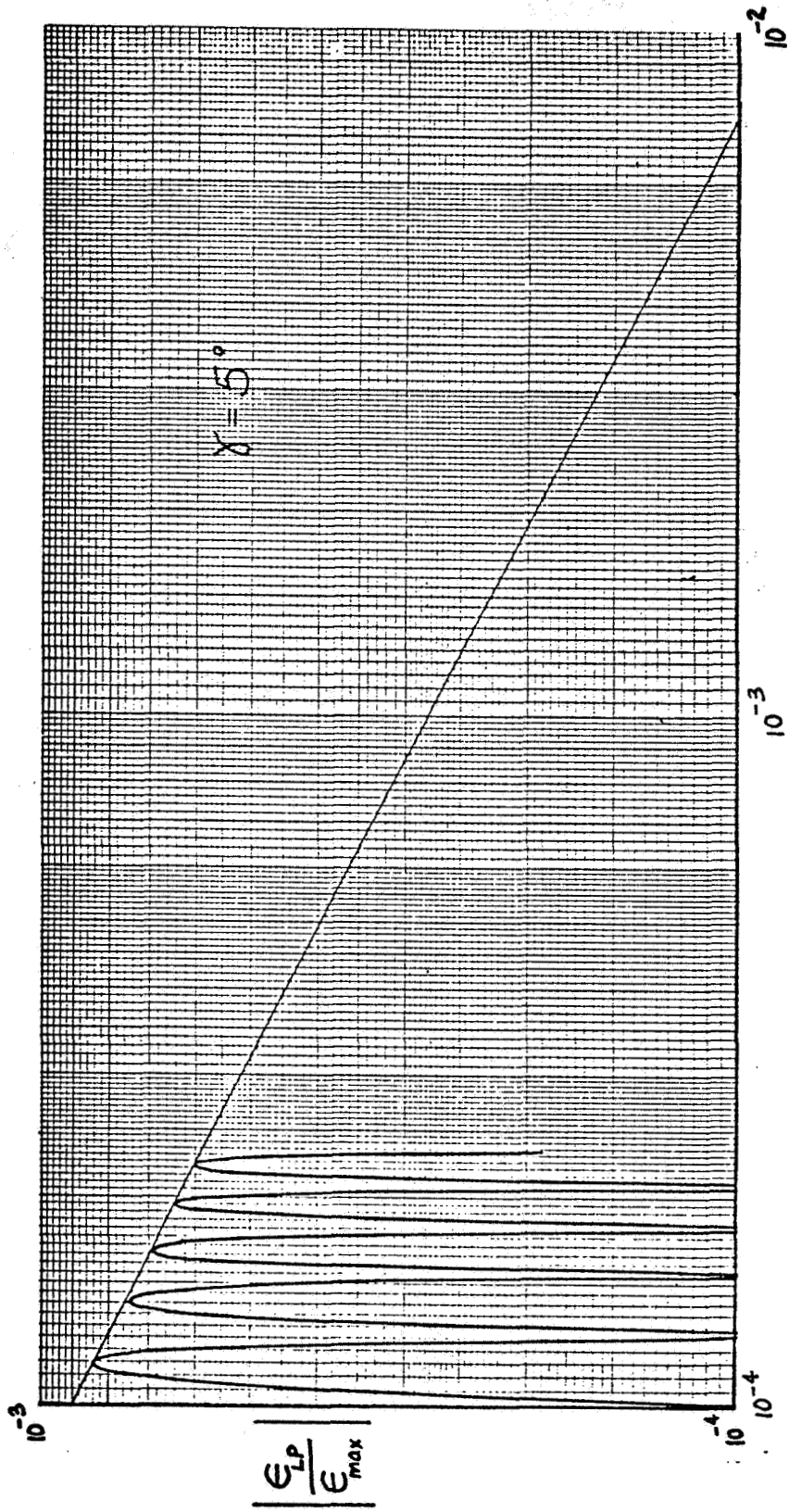
SWEEP WIDTH FACTOR q

FIGURE 14 — NORMALIZED PHASE ERROR AS A FUNCTION OF
(CONT'D) THE SWEEP WIDTH FACTOR WITH THE SATELLITE
ELEVATION ANGLE AS PARAMETER
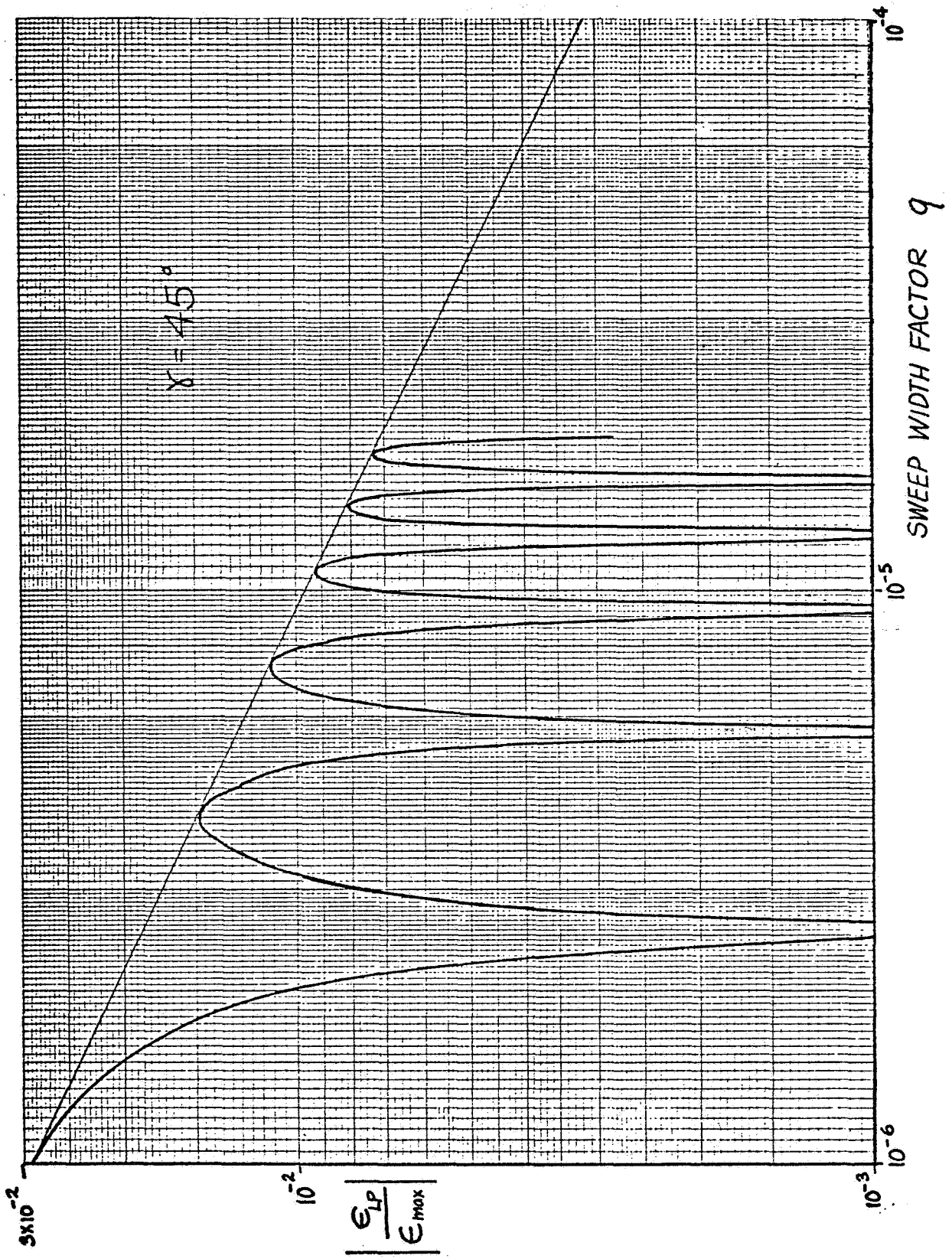
FIGURE 14 CONTINUED FOR $\gamma = 45°$
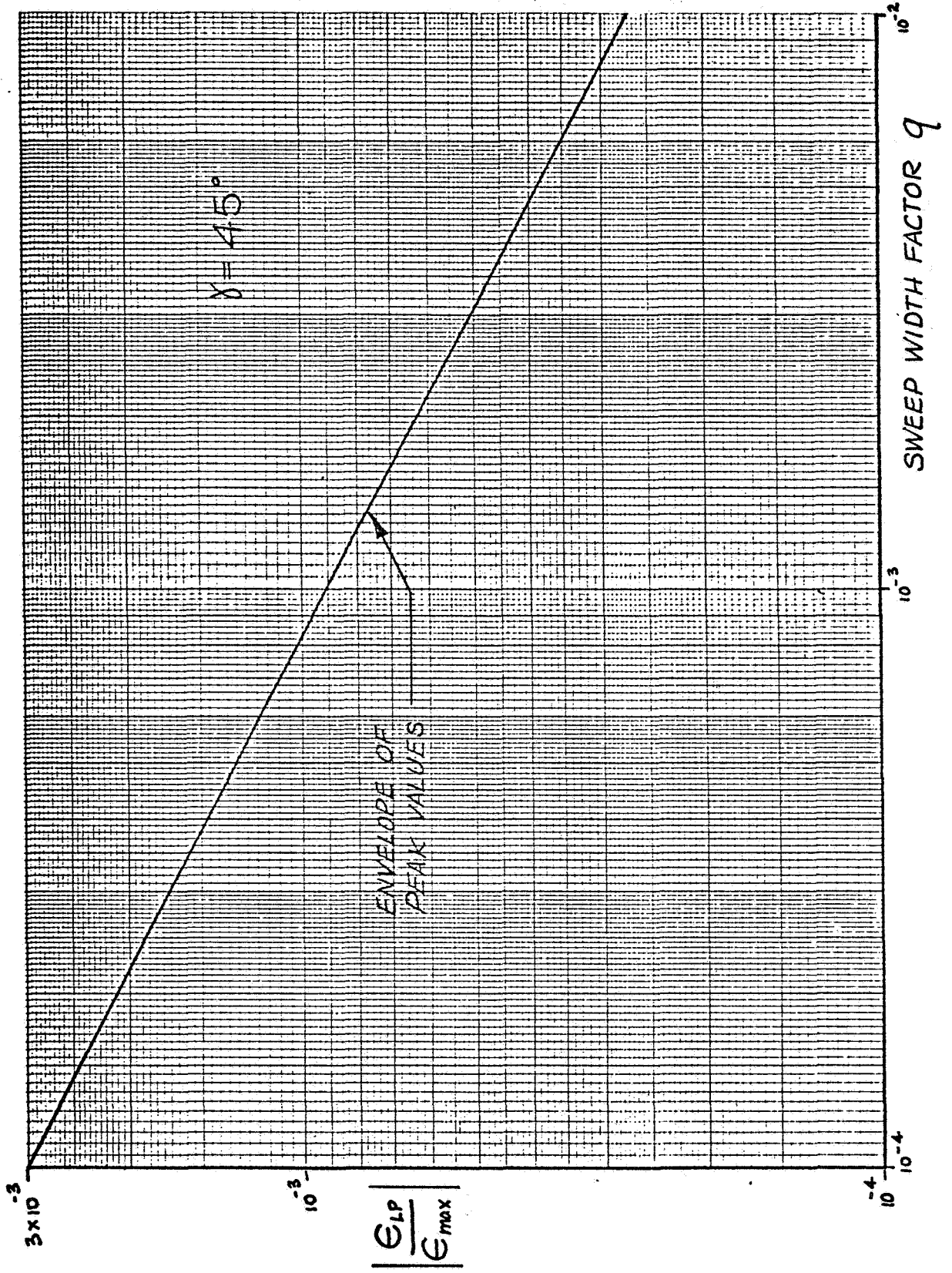
FIGURE 14 CONTINUED FOR $\gamma = 45°$
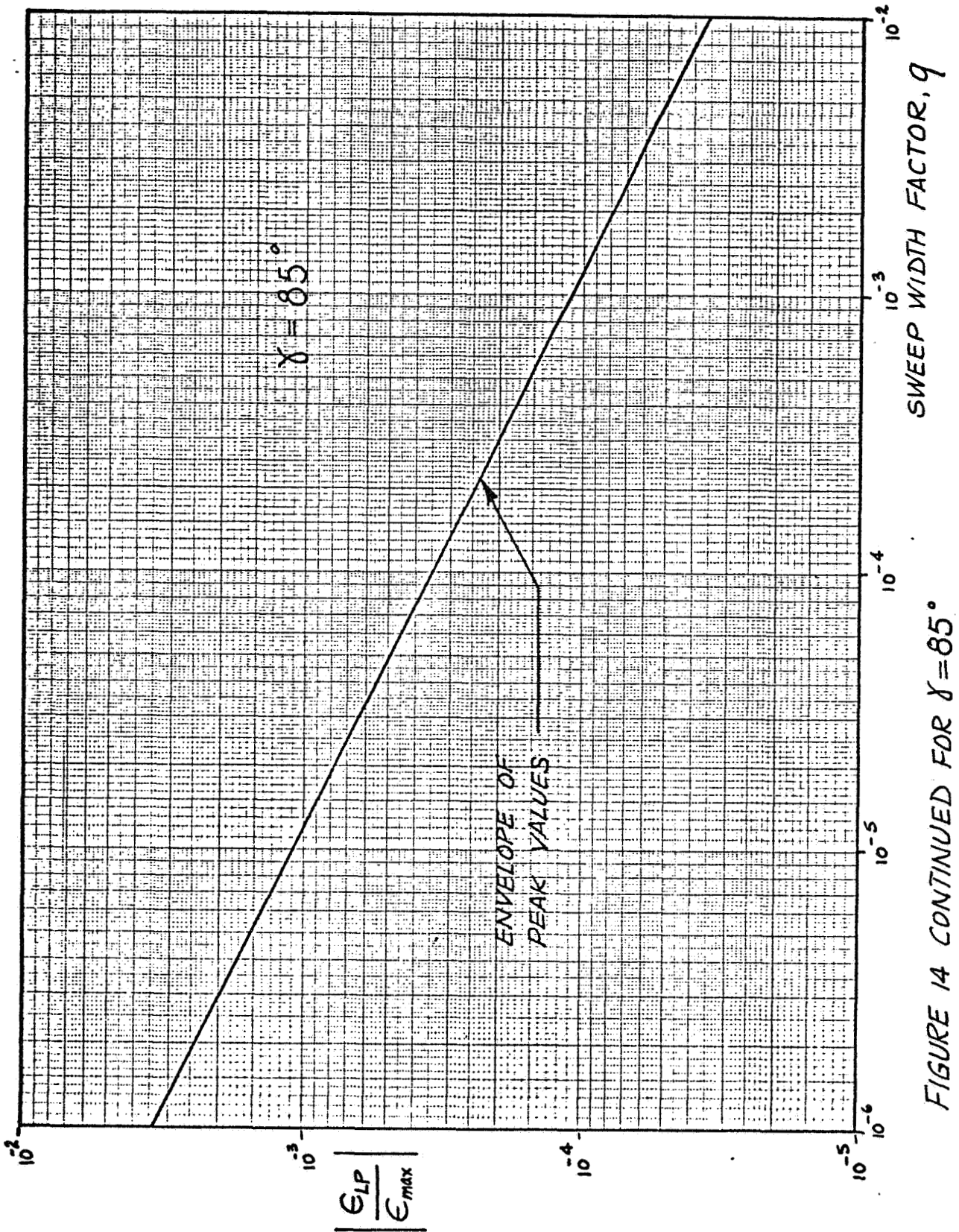
FIGURE 14 CONTINUED FOR $\gamma = 85°$

4.2 UTILIZATION OF PATH LENGTH DEPENDENCE

In this section the wavelength is assumed constant while the path lengths are allowed to vary in accordance with a user's motion during the integration time. Hence equation (8) is written

$$\Delta\alpha'(t) = \frac{2\pi L_3(t)}{\lambda} + \frac{B}{A}\left\{ \sin\left[\frac{2\pi L_1(t)}{\lambda}\right] - \sin\left[\frac{2\pi L_2(t)}{\lambda}\right] \right\}$$

where

$$L_3(t) = \ell_2 - \ell_1 \text{ , a function of time}$$

$$L_1(t) = \ell_4 - \ell_2 \text{ , a function of time}$$

$$L_2(t) = \ell_3 - \ell_1 \text{ , a function of time}$$

In this case, low-pass filtering $\Delta\alpha'(t)$ results in

$$\Delta\alpha'_{LP} = \frac{2\pi}{\lambda T} \int_0^T L_3(t)\, dt$$

$$+ \frac{B}{AT}\left\{ \int_0^T \sin\left[\frac{2\pi L_1(t)}{\lambda}\right] dt - \int_0^T \sin\left[\frac{2\pi L_2(t)}{\lambda}\right] dt \right\} \quad (23)$$

At a particular instant let the user be located at a point where

$$L_3(t) = L_{30}$$
$$L_1(t) = L_{10}$$
$$L_2(t) = L_{20}$$

Considering user motion shortly after this instant as a perturbation on these L's, it is possible to write

$$L_3(t) = L_{30} + \Delta L_3$$
$$L_1(t) = L_{10} + \Delta L_1 \qquad (24)$$
$$L_2(t) = L_{20} + \Delta L_2$$

where ΔL_i (i=1, 2, 3) are incremental path length differences.

Substituting equations (24) into (23) yields

$$\Delta \alpha'_{LP} = \frac{2\pi L_{30}}{\lambda} + \frac{2\pi}{\lambda T} \int_0^T \Delta L_3 \, dt$$
$$+ \frac{B}{AT} \left\{ \int_0^T \sin \frac{2\pi (L_{10} + \Delta L_1)}{\lambda} \, dt - \int_0^T \sin \frac{2\pi (L_{20} + \Delta L_2)}{\lambda} \, dt \right\}$$

Expanding,

$$\Delta \alpha'_{LP} = \Delta \alpha + \frac{2\pi}{\lambda T} \int_0^T \Delta L_3 \, dt$$
$$+ \frac{B}{AT} \left\{ \sin\left(\frac{2\pi L_{10}}{\lambda}\right) \int_0^T \cos\left(\frac{2\pi \Delta L_1}{\lambda}\right) dt + \cos\left(\frac{2\pi L_{10}}{\lambda}\right) \int_0^T \sin\left(\frac{2\pi \Delta L_1}{\lambda}\right) dt \right.$$
$$\left. - \sin\left(\frac{2\pi L_{20}}{\lambda}\right) \int_0^T \cos\left(\frac{2\pi \Delta L_2}{\lambda}\right) dt - \cos\left(\frac{2\pi L_{20}}{\lambda}\right) \int_0^T \sin\left(\frac{2\pi \Delta L_2}{\lambda}\right) dt \right\} \qquad (25)$$

Note that the desired phase difference information $\Delta\alpha$ appears as the first term of equation (25). It remains to investigate the magnitude of the remaining terms (the error) for practical values of T.

The user's velocity $\vec{\mathcal{N}}$ can be resolved in the four directions which are the direct and reflected signal paths (see Figure 15). Suppose that the integration time T is short enough so that velocities $\mathcal{N}_1$, $\mathcal{N}_2$, $\mathcal{N}_3$, and $\mathcal{N}_4$ may be considered constant. In such a case the distances traversed at each velocity are $\mathcal{N}_i\, t$ (i=1, 2, 3, 4). Recalling the definitions of L_1, L_2, and L_3, it follows that

$$\Delta L_1 = \left(\mathcal{N}_4 - \mathcal{N}_2\right) t$$

$$\Delta L_2 = \left(\mathcal{N}_3 - \mathcal{N}_1\right) t \qquad (26)$$

$$\Delta L_3 = \left(\mathcal{N}_2 - \mathcal{N}_1\right) t$$

Using these relations in (25) gives

$$\Delta\alpha'_{LP} = \Delta\alpha + \frac{2\pi}{\lambda}\left(\mathcal{N}_2 - \mathcal{N}_1\right)\frac{T}{2}$$

$$+ \frac{B}{AT}\left\{ \sin\left(\frac{2\pi L_{10}}{\lambda}\right) \int_0^T \cos\frac{2\pi(\mathcal{N}_4 - \mathcal{N}_2)t}{\lambda}\, dt \right.$$

$$+ \cos\left(\frac{2\pi L_{10}}{\lambda}\right) \int_0^T \sin\frac{2\pi(\mathcal{N}_4 - \mathcal{N}_2)t}{\lambda}\, dt$$

$$- \sin\left(\frac{2\pi L_{20}}{\lambda}\right) \int_0^T \cos\frac{2\pi(\mathcal{N}_3 - \mathcal{N}_1)t}{\lambda}\, dt$$

$$\left. - \cos\left(\frac{2\pi L_{20}}{\lambda}\right) \int_0^T \sin\frac{2\pi(\mathcal{N}_3 - \mathcal{N}_1)t}{\lambda}\, dt \right\} \qquad (27)$$
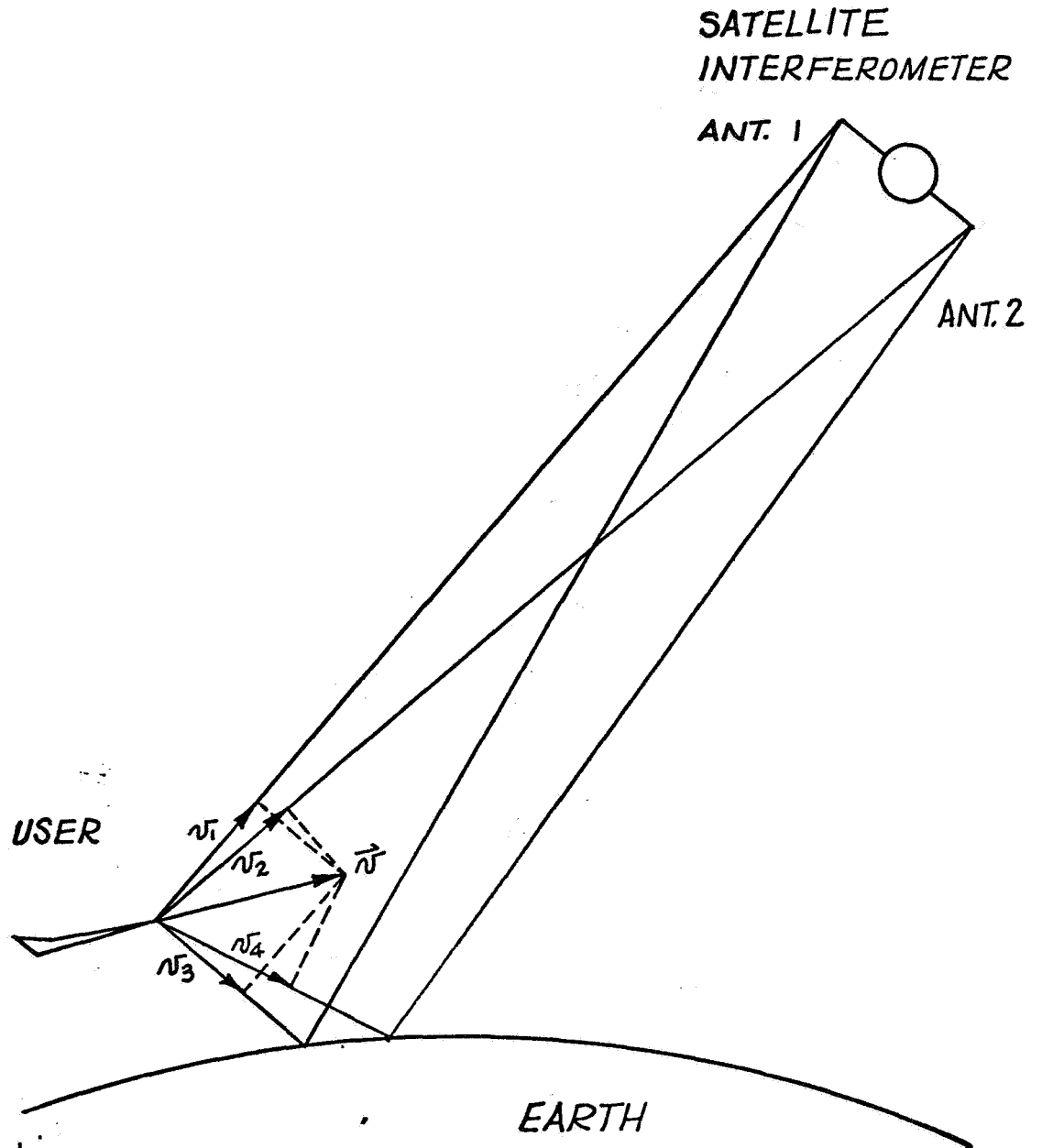
FIGURE 15 — GEOMETRY FOR MOVING USER CASE
SHOWING VELOCITY COMPONENTS

The bracketed term of (27) is bounded for all T. This term along with its factor of $\frac{B}{AT}$ can therefore be made arbitrarily small by increasing T. At the same time, the second term of (27) increases with increasing T. An overriding consideration here is that T must be smaller than the time it takes a user to travel a distance equal to the desired position determination accuracy. For position determination within a one nautical mile diameter circle, a SST traveling at 900 m/sec should not be required to integrate for more than one second. With T fixed in this way, the magnitude of the first error term of (27) can be calculated from an estimate of $\nu_2 - \nu_1$ derived as follows.

From spherical trigonometry, if $\vec{\nu}$ is the user velocity, it may be projected (through the angle δ) onto any direction using

$$\cos \delta = \cos \gamma \cos \psi$$

where γ and ψ, shown in Figure 16, are determined respectively by the interferometer antenna elevation angle and its azimuthal angle measured from $\vec{\nu}$.

Hence

$$\nu_2 = \nu \cos \gamma_2 \cos \psi_2 \quad \text{for antenna 2}$$

$$\nu_1 = \nu \cos \gamma_1 \cos \psi_1 \quad \text{for antenna 1}$$

FIGURE 16 — GEOMETRY USED TO PROJECT USER VELOCITY $\vec{u}$ IN DIRECTION OF INTERFEROMETER ANTENNA

Now

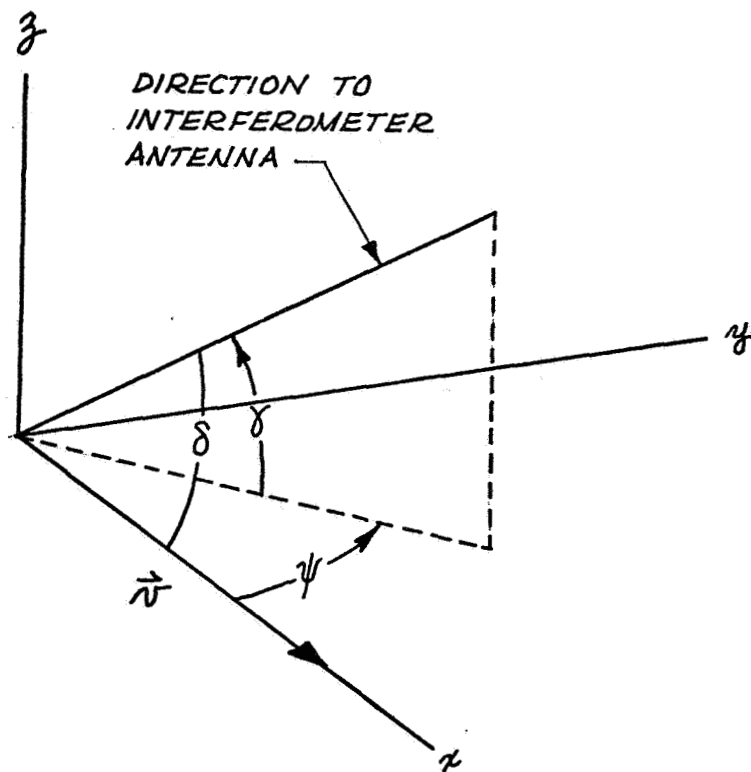$$u_2 - u_1 = u\left(\cos\gamma_2 \cos\psi_2 - \cos\gamma_1 \cos\psi_1\right)$$

but $\gamma_1 = \gamma_2 + \Delta\gamma$ and $\psi_1 = \psi_2 + \Delta\psi$

therefore

$$u_2 - u_1 = u\left[\cos\gamma_2 \cos\psi_2 - \cos(\gamma_2 + \Delta\gamma)\cos(\psi_2 + \Delta\psi)\right]$$

$$= \mathcal{V} \left\{ \cos \gamma_2 \cos \psi_2 - \left[\left(\cos \gamma_2 \cos \Delta\gamma - \sin \gamma_2 \sin \Delta\gamma \right) \cdot \left(\cos \psi_2 \cos \Delta\psi - \sin \psi_2 \sin \Delta\psi \right) \right] \right\}$$

$$\approx \mathcal{V} \left[\cos \gamma_2 \cos \psi_2 - \left(\cos \gamma_2 - \Delta\gamma \sin \gamma_2 \right) \left(\cos \psi_2 - \Delta\psi \sin \psi_2 \right) \right]$$

$$\approx \mathcal{V} \left[\Delta\gamma \sin \gamma_2 \cos \psi_2 + \Delta\psi \sin \psi_2 \cos \gamma_2 \right]$$

but $\quad \Delta\gamma \approx \Delta\psi \quad$ therefore

$$\mathcal{V}_2 - \mathcal{V}_1 \approx \mathcal{V}(\Delta\gamma) \sin (\gamma_2 + \psi_2) \leq \mathcal{V}(\Delta\gamma)$$

Now

$$\frac{\pi(\mathcal{V}_2 - \mathcal{V}_1) T}{\lambda} \leq \frac{\pi \mathcal{V}(\Delta\gamma)}{\lambda} = 1.5 \times 10^{-3} \qquad (28)$$

at L-band for a 20λ baseline synchronous altitude interferometer. Since a one nautical mile accuracy corresponds to a phase measurement made to within 0.006 radian, the first error term of (27) will be ignored.

The remaining velocity differences appearing in (27) can be estimated from the following analysis based on Figure 17. Assuming a user in level flight at velocity $\vec{\mathcal{V}}$, $\mathcal{V}_2' = \mathcal{V} \cos \psi_2$ is the user's rate of horizontal travel in the plane of the signal paths. The components of $\mathcal{V}_2'$ along the direct and reflected signal paths
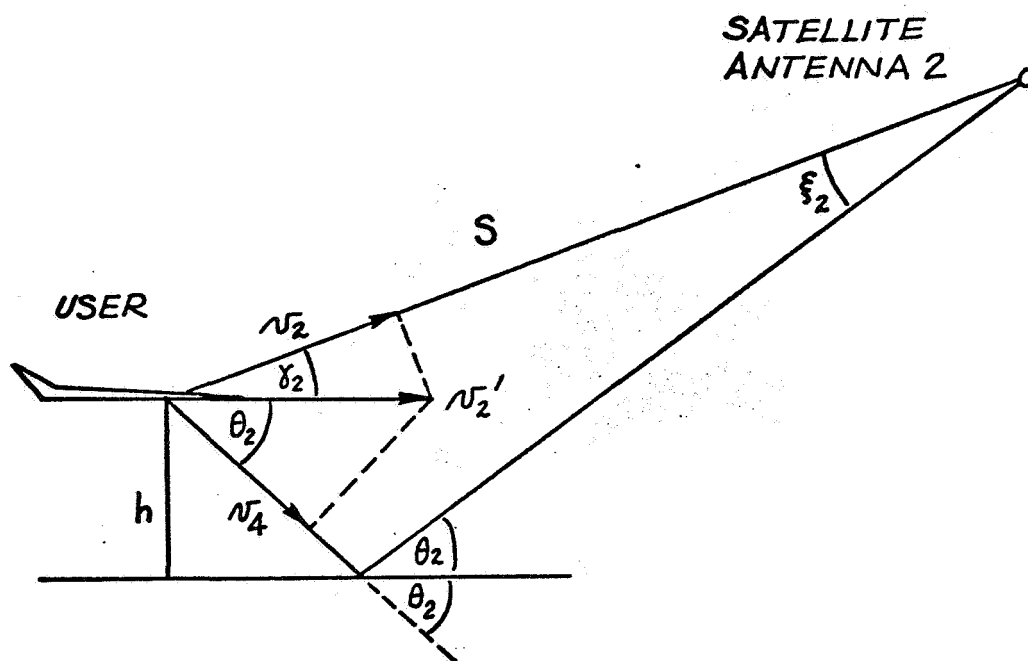
FIGURE 17 (a) — SYSTEM GEOMETRY SIDE VIEW
SHOWING ONE ANTENNA
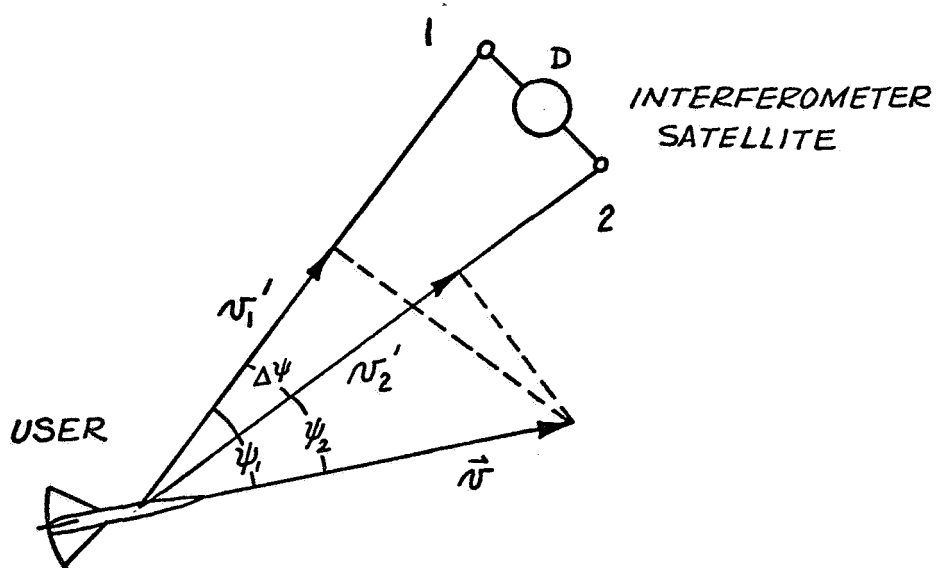
FIGURE 17 (b) — TOP VIEW OF FIGURE 17(a)

are N_2 and N_4 respectively.

$$N_4 = N_2' \cos \theta_2 = N \cos \psi_2 \cos \theta_2$$

$$N_2 = N_2' \cos \gamma_2 = N \cos \psi_2 \cos \gamma_2$$

From Figure 17 (a) $\quad \theta_2 = \xi_2 + \gamma_2 \approx \dfrac{h}{S} + \gamma_2$

therefore

$$N_4 = N \cos \psi_2 \cos \left(\dfrac{h}{S} + \gamma_2 \right)$$

$$= N \cos \psi_2 \left[\cos \dfrac{h}{S} \cos \gamma_2 - \sin \dfrac{h}{S} \sin \gamma_2 \right]$$

$$\approx N \cos \psi_2 \left[\cos \gamma_2 - \dfrac{h}{S} \sin \gamma_2 \right]$$

and

$$N_4 - N_2 = -N \cos \psi_2 \left[\dfrac{h}{S} \sin \gamma_2 \right] \tag{29}$$

Similarly for antenna 1

$$N_3 - N_1 = -N \dfrac{h}{S} \cos \psi_1 \sin \gamma_1$$

but $\quad \gamma_1 = \gamma_2 + \Delta\gamma$, therefore

$$N_3 - N_1 = -N \dfrac{h}{S} \cos \psi_1 \sin (\gamma_2 + \Delta\gamma)$$

$$= -N \dfrac{h}{S} \cos \psi_1 \left[\sin \gamma_2 \cos \Delta\gamma + \cos \gamma_2 \sin \Delta\gamma \right]$$

$$\approx -N \dfrac{h}{S} \cos \psi_1 \left[\sin \gamma_2 + \Delta\gamma \cos \gamma_2 \right] \tag{30}$$

In estimating the magnitude of the velocity differences, assume that the user travels perpendicular to the plane of the first antenna's signal paths (this may be true for most of a transatlantic flight). Hence let $\psi_1 = 90°$ in which case $(\mathcal{N}_3 - \mathcal{N}_1) = 0$. ψ_1 and ψ_2 differ by the azimuthal angular antenna separation $\Delta\psi = \psi_1 - \psi_2$. Therefore $\psi_2 = 90° - \Delta\psi$.

Now $\mathcal{N}_4 - \mathcal{N}_2 = -\mathcal{V}(\sin \Delta\psi)\dfrac{h}{s} \sin \gamma_2$

From Figure 18, γ_2 might typically be $40°$ for a transatlantic flight while $\sin \Delta\psi \approx \dfrac{D}{S} = 10^{-7}$ radian as discussed in section 4.1.2. For a 900 m/sec SST at 65,000 feet and a 20λ, L-band, synchronous interferometer

$$\left| \mathcal{N}_4 - \mathcal{N}_2 \right| = 3 \times 10^{-7} \text{ m/sec} \tag{31}$$

With $\left| \mathcal{N}_3 - \mathcal{N}_1 \right| = 0$, (27) becomes

$$\Delta\alpha'_{LP} = \Delta\alpha + \frac{\pi(\mathcal{N}_2 - \mathcal{N}_1)T}{\lambda}$$

$$+ \frac{B}{AT}\left\{ \sin\left(\frac{2\pi L_{10}}{\lambda}\right) \int_0^T \cos \frac{2\pi(\mathcal{N}_4 - \mathcal{N}_2)t}{\lambda} dt \right.$$

$$+ \cos\left(\frac{2\pi L_{10}}{\lambda}\right) \int_0^T \sin \frac{2\pi(\mathcal{N}_4 - \mathcal{N}_2)t}{\lambda} dt$$
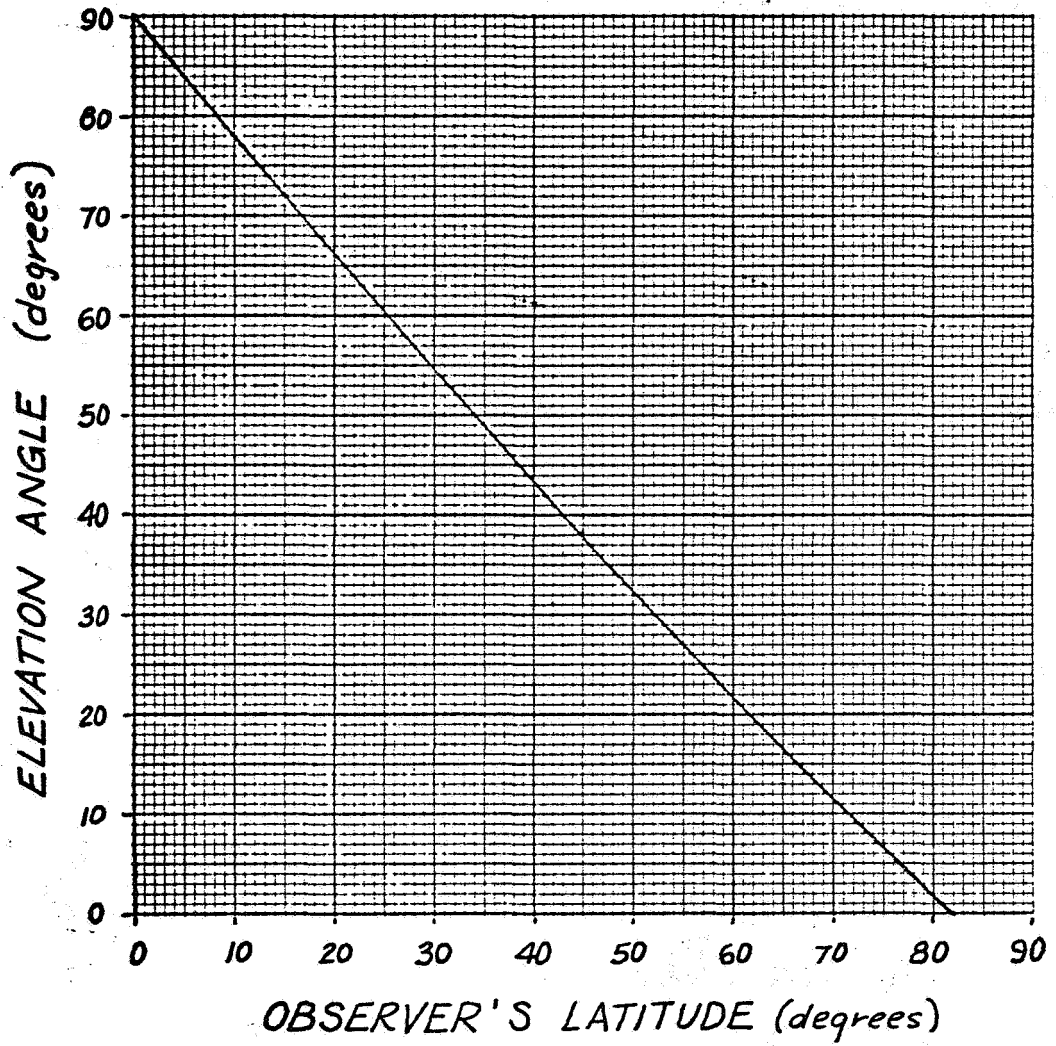
$$\left. - \sin\left(\frac{2\pi L_{20}}{\lambda}\right) \cdot T \right\}$$

FIGURE 18 — ELEVATION ANGLE FOR SYNCHRONOUS SATELLITE ON OBSERVER'S MERIDIAN

$$= \Delta\alpha + \frac{\pi(\nu_2 - \nu_1)T}{\lambda}$$

$$+ \frac{B}{AT}\left\{\sin\left(\frac{2\pi L_{10}}{\lambda}\right)\left[\frac{\lambda}{2\pi(\nu_4 - \nu_2)}\right]\sin\left[\frac{2\pi(\nu_4 - \nu_2)T}{\lambda}\right]\right.$$

$$+ \cos\left(\frac{2\pi L_{10}}{\lambda}\right)\left[\frac{\lambda}{2\pi(\nu_4 - \nu_2)}\right]\left[1 - \cos\frac{2\pi(\nu_4 - \nu_2)T}{\lambda}\right]$$

$$\left. - \sin\left(\frac{2\pi L_{20}}{\lambda}\right)\cdot T\right\} \tag{32}$$

Considering (28) and (31) with $T = 1$ second, $\Delta\alpha'_{LP}$ is approximated by

$$\Delta\alpha'_{LP} = \Delta\alpha + \frac{B}{A}\left[\sin\left(\frac{2\pi L_{10}}{\lambda}\right) - \sin\left(\frac{2\pi L_{20}}{\lambda}\right)\right] \tag{33}$$

Recalling that L_{10} and L_{20} are fixed path length differences which are quite small,

$$\Delta\alpha' \approx \Delta\alpha + \frac{2\pi}{\lambda}\cdot\frac{B}{A}\left(\mathscr{L}_1 - \mathscr{L}_2\right) \tag{34}$$

where $\mathscr{L}_1 - \mathscr{L}_2$ is given by Figure 13. The normalized error in this case is

$$\left|\frac{\epsilon_{LP}}{\epsilon_{max}}\right| = \frac{\pi}{\lambda}\left|\mathscr{L}_1 - \mathscr{L}_2\right| \tag{35}$$

At $\gamma = 40°$, $\left| \alpha_1 - \alpha_2 \right| = 3 \times 10^{-3}$ m from Figure 13 with $h = 2 \times 10^4$ m and $\Delta \gamma = 10^{-7}$ radian. Hence

$$\left| \frac{\epsilon_{LP}}{\epsilon_{max}} \right| = 0.049 \quad \text{at} \quad 1600 \text{ MHz}$$

Assuming $\frac{B}{A} = 0.1$, $\left| \epsilon_{LP} \right| = 0.0098$ radian. Using equation (1), this value of phase difference can be converted to an error in angular position.

$$\left| \epsilon_{LP} \right| = \frac{2\pi D}{\lambda} \cos \theta = \frac{2\pi D}{\lambda} \sin (90° - \theta)$$

But $81° \leq \theta \leq 90°$ when viewing the earth from synchronous altitude.

Hence

$$\left| \epsilon_{LP} \right| \approx \frac{2\pi D}{\lambda} \left(\frac{\pi}{2} - \theta \right)$$

$$\approx \frac{2\pi D}{\lambda} \cdot \frac{\Delta x}{S}$$

where Δx is the radius of the user's circle of possible positions and S is the satellite slant range. Using $\left| \epsilon_{LP} \right| = 0.0098$ radian,

$$\Delta x = 2.8 \text{ km}$$

5.0   DISCUSSION AND CONCLUSIONS

The equation for the phase measurement made by a satellite interferometer has been derived to reveal the multipath error contribution. A means for reducing this error has been presented for phase-coherent reflected energy as occurs in a specular situation.[*] The error reducing principle involves allowing or forcing the multipath - direct signal phase relationship to vary during which a time averaging is used to extract a more accurate phase measurement. The multipath - direct signal phase relationship is forced to vary by sweeping the operating frequency. Alternatively, for a moving user, it can simply be allowed to vary with user motion over the period of integration.

In the frequency sweep case, the final error depends upon the amount of sweep defined by the sweep width factor q . Figure 14 shows the effect of q on

---

[*]   Reflection from a changing surface such as the sea may be diffuse and time varying. It may cause the indirectly received wave to vary somewhat in amplitude and phase during the integration interval proposed here. Both of these variations cause a time variation in the measured phase of the resultant received wave. However, the variation of the latter may, in fact, aid in the process of cancelling the error.

the multipath error for q between 10^{-5} and 10^{-2} and for three elevation angles. This figure shows that there exists a large number of critical values of q for which the error vanishes. These zeros of equation (22) occur for q satisfying

$$q \; \frac{J_1(2\pi f_0 q \tau)}{J_0(2\pi f_0 q \tau)} \; = \; \cot \left(2\pi f_0 \tau\right)$$

The zeros occur more frequently as q increases and also for increasing elevation angle. Where the zeros occur extremely close together in Figure 14, only the envelope of the maximum error points is shown.

From the standpoint of spectrum conservation, the smallest zero of (22) should be selected as the operating point since $2q f_0$ gives the sweep width. However, should the user move substantially during the time interval of measurement, the zeros of (22) will shift slightly. In this case a q should be selected out along the tail of Figure 14 based on the maximum tolerable error for a desired navigation accuracy. Operation above this "cutoff" value of q will give an error value less than the maximum one allowed.

For the case of integration while the user is in motion, a maximum integration time of one second

has been established. This insures that the user can make a position measurement before having moved outside a one nautical mile diameter circle about his calculated position. Using the same satellite and operating frequency as in the frequency-sweep case, the integration-while-in-motion technique for $T = 1$ second results in a position error of about 2.8 km for a SST at 65,000 feet. This is not as good as results achievable with the frequency-sweep technique which would give a 0.057 km accuracy for $q = 10^{-3}$ (a 3.2 MHz sweep at L-band) assuming such accuracies are compatible with the precision of electrical phase measuring equipment. The integration-while-in-motion technique does not require transmitter sweeping circuits or elaborate receiver tracking. However, slow moving users will not be able to use this method for multipath reduction when measuring over a short period of time.

BIBLIOGRAPHY

1. Institute for Defense Analysis, "The North
    Atlantic Air-Traffic Control System," FAA
    Report No. RD 65-96, September 1965.

2. Westinghouse Defense and Space Center,
    "Interferometer Ground Test of a System for
    Measuring Angles from Satellites," Technical
    Proposal, March 24, 1965.

3. Westinghouse Defense and Space Center,
    "Navigation Satellite System," Final Report on
    NASA Contract No. NASw-785, Phase I, January 30,
    1964.

4. Westinghouse Defense and Space Center,
    "Navigation Satellite System," Final Report on
    NASA Contract No. NASw-785, Phase II, October 15,
    1964.

5. Westinghouse Defense and Space Center,
    "Navigation / Traffic Control Techniques Exper-
    iment Study," Final Report on NASA Contract No.
    NASw-1387, September 1966.

6. Keats, E. S., "A Navigation System Using Distance and Direction Measurements from a Satellite," Navigation, Vol. 11, No. 3, Autumn 1964, pp. 335-341.

7. Keats, E. S., "A New Concept for a Navigation Satellite System," Westinghouse Engineer, Vol. 24, July 1964, pp. 105-109.

8. Cubic Corporation, "Feasibility Study for a Vehicle Attitude Determining System," Final Report No. RADC-TDR-64-318 (Vol. I and II) on U. S. Air Force Contract No. AF 30(602)-3135, November, 1964.

9. Cubic Corporation, "RF Interferometer Attitude Sensor for ATS-4," Proposal No. P-66080, August 8, 1966.

10. Cubic Corporation, "Space SECOR (SEquential COllation of Range) Report No. P-63086, July 18, 1963.

11. Klein, P. I., "Analysis of a Short-Baseline
    Radiating Interferometer Navigation Satellite
    Concept Incorporating Methods to Eliminate
    Systematic Navigation Error," University of
    Pennsylvania, Philadelphia, Pennsylvania, The
    Moore School of Electrical Engineering Report
    No. 68-26, May 1968.

12. Klein, P. I., "Analysis of a Synthetic Aperture
    Radiating Interferometer Navigation Satellite
    Concept," University of Pennsylvania, Philadelphia,
    Pennsylvania, The Moore School of Electrical
    Engineering Report No. 69-03, May 1969.

13. Reid, J. H., "The SECOR Approach to Coordinate
    Determination for Ships and Aircraft," Navigation,
    Vol. 11, No. 4, January 1965, pp. 393-416.

14. Keats, E. S., "Navigational Satellites: Beacons
    for Ships and Planes," Electronics, Vol. 38,
    February 8, 1965, pp. 79-86.

15. Dougherty, H. T., "A Survey of Microwave Fading Mechanisms Remedies and Applications," ESSA Technical Report ERL 69-WPL 4, March 1968.

16. Beckmann, P. and A. Spizzichino, _The Scattering of Electromagnetic Waves from Rough Surfaces_, The Macmillan Company, New York, 1963.

17. Kerr, D. E., _Propagation of Short Radio Waves_, Boston Technical Publishers, Inc., Lexington, Mass., 1964.

18. Duncan, J. W., "The Effect of Ground Reflections and Scattering on an Interferometer Direction Finder," IEEE Transactions on Aerospace and Electronic Systems, Vol. AES-3, No. 6, November 1967, pp. 922-932.

19. Sherwood, E. M. and E. L. Ginzton, "Reflection Coefficients of Irregular Terrain at 10 cm," Proc. IRE, Vol. 43, No. 7, July 1955, pp. 877-878.

20. Jordan, K. L., "Measurement of Multipath Effects in a Satellite-Aircraft UHF Link," Proceedings Letters, Proc. IEEE, June 1967, pp. 1117-1118.

21. McGavin, R. E. and L. J. Maloney, "Study at 1046
    Megacycles per Second of the Reflection Coef-
    ficient of Irregular Terrain at Grazing Angles,"
    Jour. Res. NBS, Vol. 63D, 1959, pp. 235-248.

DISTRIBUTION LIST

for report: "Reducing Multipath Error in an Angle-Measuring
Navigation Satellite System"

under NASA Grant NGR-39-010-087

by

University of Pennsylvania

Addressee	Copies

National Aeronautics and Space Administration
Washington, D. C. 20546
   Attn: Eugene Ehrlich, Chief, Navigation and
        Traffic Control Programs, Code SCN
	5

Winnie M. Morgan, Code US	5 (+Repro.)
Electronics Research Center National Aeronautics and Space Administration 575 Technology Square Cambridge, Massachusetts 02139 Attn: Leo Keane, Code GSE	1

Goddard Space Flight Center
National Aeronautics and Space Administration
Greenbelt, Maryland 20771
   Attn: Charles R. Laughlin, Code 733
        Marvin Maxwell, Code 731
	1
	1

Director of Defense Research and Engineering Office of the Secretary of Defense Pentagon, Washington, D. C. 20310 Attn: Asst. Director (Communication and Electronics)	1
Department of the Navy Naval Air Systems Command Washington, D. C. 20360 Attn: Astronautics Division	1
U. S. Coast Guard 13th and E Street, N. W. Washington, D. C. 20591 Attn: Aids to Navigation Division	1
Office of Research and Development Maritime Administration Washington, D. C. Attn: Charles Kurz	1

Addressee	Copies

Langley Research Center
National Aeronautics and Space Administration
Hampton, Virginia
   Attn: Mr. Fred Morel   1

Federal Aviation Agency
800 Independence Avenue, S. W.
Washington, D. C. 20553
   Attn: Alexander Winick, Chief,   1
       Navigation Division, RD 300
       Communication Division, RD 200   1

National Aviation Facilities Experimental Center
Federal Aviation Agency
Atlantic City, New Jersey
   Attn: Nathanial Braverman   1

The Rand Corporation
1700 Main Street
Santa Monica, California 90406
   Attn: J. Hutcheson   1

Stanford Research Institute
Menlo Park, California 94025
   Attn: D. R. Scheuch   1

Johns Hopkins Applied Physics Laboratory
8621 Georgia Avenue
Silver Spring, Maryland 20910
   Attn: Dr. Robert Newton   1

Lincoln Laboratory
Massachusetts Institute of Technology
Lexington, Massachusetts 02173
   Attn: Dr. Thomas Goblick   1

The Boeing Company
Aero-Space Division
Seattle, Washington   1

General Electric Company
Advanced Technology Laboratories
P. O. Box 43
Schenectady, New York 12301
   Attn: Roy Anderson   1

International Business Machines Corporation
Federal Systems Division
18100 Frederick Pike
Gaithersburg, Maryland 20760

Philco-Ford Corporation
Western Development Laboratories
3825 Fabian Way
Palo Alto, California
   Attn: Reiss Jensen   1

Addressee	Copies
TRW Systems One Space Park Redondo Beach, California 90278 Attn: David Otten	1
Radio Corporation of America Defense Electronic Products Systems Engineering, Evaluation and Research, 127-310 Moorestown, New Jersey 08057 Attn: Mike Mitchell	1

Hughes Aircraft Company
Aerospace Group
Culver City, California 90232
  Attn: Guidance and Controls
         Division, R. S. Boucher
	1

Westinghouse Electric Company Defense Space Center/Aerospace Division Box 746 Baltimore, Maryland 21203 Attn: Ed Keats	1
Cubic Corporation 9233 Balboa Avenue San Diego, California 92123 Attn: James Reid	1
University of Michigan Institute of Science and Technology Willow Run Laboratories Ann Arbor, Michigan 48103 Attn: G. Casserly	1

U. S. Naval Research Laboratory
Washington, D. C. 20390
  Attn: Roger Easton, Code 5160
         Leo Young, Code 5403
	1
	1

Aerospace Corporation Los Angeles, California Attn: Dr. Philip Diamond	1
Stanford Research Institute 1611 N. Kent Street Arlington, Virginia 22209 Attn: J. Clemens	1

Addressee	Copies

Communications and Systems, Inc.
6565 Arlington Boulevard
Falls Church, Virginia   22046
  Attn: Neil MacGregor   1

U. S. Army Electronics Command
Avionics Laboratory, AMSEL-VL-N
Fort Monmouth, New Jersey   07703
  Attn: Les Lang   1
         Tom Daniels   1

Communications Satellite Corporation
950 L'Enfant Plaza So., S. W.
Washington, D. C.   20024
  Attn: Ed Martin   1

Tom Benham
Haverford College
5 College Lane
Haverford, Pennsylvania   1

Donald Jansky
Office of Telecommunications Management
Executive Office of the President
Washington, D. C.   20504   1

Perry I. Klein
Communications Satellite Corporation
950 L'Enfant Plaza So., S. W.
Washington, D. C.   20024   20

Dr. F. Haber   1

R. Hrusovsky MS62
RCA Defense Electronics Products
Astro Electronics Division
P. O. Box 800
Princeton, New Jersey   08540   10

G. Thomas   1

R. Lefferts   1

Dr. H. Kritikos   1

DOCUMENT CONTROL DATA - R & D

(Security classification of title, body of abstract and indexing annotation must be entered when the overall report is classified)

1. ORIGINATING ACTIVITY *(Corporate author)*	2a. REPORT SECURITY CLASSIFICATION
University of Pennsylvania Moore School of Electrical Engineering Philadelphia, Pennsylvania 19104	UNCLASSIFIED
	2b. GROUP

3. REPORT TITLE

REDUCING MULTIPATH ERROR IN AN ANGLE-MEASURING NAVIGATION SATELLITE SYSTEM

4. DESCRIPTIVE NOTES *(Type of report and inclusive dates)*

Interim Technical Report

5. AUTHOR(S) *(First name, middle initial, last name)*

RICHARD A. HRUSOVSKY

6. REPORT DATE	7a. TOTAL NO. OF PAGES	7b. NO. OF REFS
September 1969	79	21

8a. CONTRACT OR GRANT NO.	9a. ORIGINATOR'S REPORT NUMBER(S)
NGR-39-010-087	Moore School Report #70-07
b. PROJECT NO.	
c.	9b. OTHER REPORT NO(S) *(Any other numbers that may be assigned this report)*
d.	

10. DISTRIBUTION STATEMENT

Distribution of this document is unlimited.

11. SUPPLEMENTARY NOTES	12. SPONSORING MILITARY ACTIVITY
	National Aeronautics and Space Admin. Space Applications Programs Office Washington, D. C. 20546

13. ABSTRACT

A major error in navigational position fixing using a satellite-borne interferometer is due to multipath propagation. Reflections, principally from the earth's surface, contaminate the phase measurement which provides positional information. A signal design method of reducing multipath error is investigated wherein the navigation signals are swept in frequency. A time averaging of the frequency-swept signals at the navigation receiver can then be used to reduce the multipath error contribution below the maximum fixed-frequency error. Since electrical phase is path length as well as wavelength dependent, the motion of a navigating user can be substituted for the transmitter sweeping provided appropriate receiver integration time is employed. (U)

14. KEY WORDS	LINK A		LINK B		LINK C	
	ROLE	WT	ROLE	WT	ROLE	WT
Navigation satellite system						
Interferometer satellite						
Multipath error						
Multipath reflections						
Multipath reflection coefficient						
Frequency-swept signals						
Integrated phase measurements						

DD FORM 1 NOV 65 **1473** (BACK)

S/N 0101-807-6821

A-31409